

Accepted Manuscript

Re-assessing the European lithium resource potential – A review of *hard-rock* resources and metallogeny

B. Gourcerol, E. Gloaguen, J. Melleton, J. Tuduri, Xavier Galiegue

PII: S0169-1368(18)30801-1

DOI: <https://doi.org/10.1016/j.oregeorev.2019.04.015>

Reference: OREGEO 2903

To appear in: *Ore Geology Reviews*

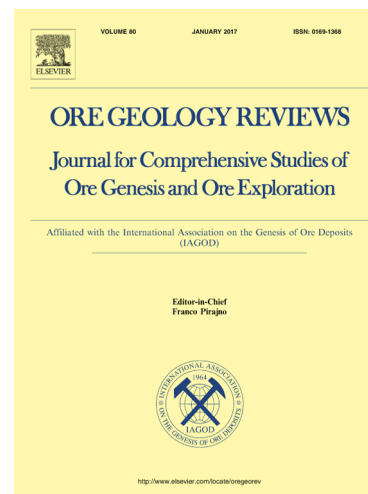
Received Date: 20 September 2018

Revised Date: 15 April 2019

Accepted Date: 23 April 2019

Please cite this article as: B. Gourcerol, E. Gloaguen, J. Melleton, J. Tuduri, X. Galiegue, Re-assessing the European lithium resource potential – A review of *hard-rock* resources and metallogeny, *Ore Geology Reviews* (2019), doi: <https://doi.org/10.1016/j.oregeorev.2019.04.015>

This is a PDF file of an unedited manuscript that has been accepted for publication. As a service to our customers we are providing this early version of the manuscript. The manuscript will undergo copyediting, typesetting, and review of the resulting proof before it is published in its final form. Please note that during the production process errors may be discovered which could affect the content, and all legal disclaimers that apply to the journal pertain.



1 Re-assessing the European lithium resource 2 potential – A review of *hard-rock* resources 3 and metallogeny

4 B. Gourcerol^{a,b*}, E. Gloaguen^c, J. Melleton^b, J. Tuduri^c, Xavier Galiegue^a

5 ^a Laboratoire d'Economie d'Orléans, Université d'Orléans, UMR7322 Faculté de Droit d'Economie et
6 de Gestion Rue de Blois - BP 26739 45067 ORLEANS Cedex 2, France

7 ^b BRGM, F-45060 Orléans, France

8 ^c ISTO, UMR 7327, Université d'Orléans, CNRS, BRGM, F-45071 Orléans, France

9 *Corresponding author: gourcerol.blandine@gmail.com

10 Graphical Abstract

11 Highlights:

- 12 • Lithium is not rare in Europe and is well represented in different orogenic settings;
- 13 • A pre-existing Li-rich source is required for Li-enrichment processes;
- 14 • Lithospheric thickening may reflect a favorable process for concentrating Li;
- 15 • Extensional geodynamical settings appear favorable for Li enrichment.

16 **Keywords:** lithium, metallogeny, pegmatite, Europe, resources

17

18 Abstract

19 Lithium, which is an excellent conductor of heat and electricity, became a strategic metal in the past
20 decade due to its widespread use in electromobility and green technologies. The resulting significant
21 increase in demand has revived European interest in lithium mining, leading several countries to
22 assess their own resources/reserves in order to secure their supplies. In this context, we present for the
23 first time a geographically-based and geological compilation of European lithium *hard-rock*
24 occurrences and deposits with their corresponding features (e.g., deposit types, Li-bearing minerals, Li
25 concentrations), as well as a systematic assessment of metallogenic processes related to lithium
26 mineralization. It appears that lithium is well represented in various deposit types related to several
27 orogenic cycles from Precambrian to Miocene ages. About thirty hard-rock deposits have been
28 identified, mostly resulting from endogenous processes such as lithium-cesium-tantalum (LCT)
29 pegmatites (e.g., Sepeda in Portugal, Aclare in Ireland, Lännta in Finland), rare-metal granites (RMG;

30 Beauvoir in France, Cinovec in the Czech Republic) and greisen (Cligga Head, Tregonning-
31 Godolphin, Meldon in the UK and Montebrias in France). Local exogenous processes may result in
32 significant Li- enrichment, such as jadarite precipitation in the Jadar Basin (Serbia), but they are rarely
33 related to economic lithium grades such as in Mn-(Fe) deposits, or in bauxite. We also identified major
34 common parameters leading to Li enrichment: 1) a pre-existing Li-bearing source; 2) the presence of
35 lithospheric thickening, which may be a favorable process for concentrating Li; 3) a regional or local
36 extensional regime; and 4) the existence of fractures acting as channel ways for exogenous processes.
37 Furthermore, we point out the heterogeneity of knowledge for several orogenic settings, such as the
38 Mediterranean orogens, suggesting either a lack of exploration in this geographical area, or significant
39 changes in the orogenic parameters.

40

41 1. Introduction

42 Over the past decade, lithium has become a strategic metal due to its physical and chemical properties,
43 being the lightest solid element and an excellent conductor of heat and electricity. This makes it an
44 excellent candidate for electromobility and green technologies, such as Li-ion batteries and other
45 energy-storage devices (Armand and Tarascon, 2008; Tarascon, 2010; Ziemann et al., 2012;
46 Manthiram et al., 2017). As a result, Li demand has increased significantly and a “lithium rush” is
47 currently happening world wide (e.g., Roskill Information Services Ltd., 2016). In this context, the
48 identification and assessment of lithium mineral resources and -reserves is a crucial step, as is
49 understanding lithium metallogeny, a major subject for discovering new mineral resources.

50 Historically, two distinct deposit types are identified: 1) *brine* deposits in which the lithium
51 grade is about 0.1% Li₂O; and 2) *hard-rock* deposits where the lithium grade generally varies from 0.6
52 to 1.0% Li₂O hosted by various Li-bearing minerals (Kesler et al., 2012; Mohr et al., 2012).

53 The brine-deposit type refers to relatively recent (mostly Quaternary), enclosed, tectonically
54 active basins that contain Li-rich lacustrine evaporites. These are produced by high evaporation rates
55 in an arid to hyper-arid climate and/or by various water inputs such as groundwater and spring water
56 circulation (e.g., Ericksen and Salas, 1987; Bradley et al., 2013). In these deposits, the Li source and
57 enrichment processes are specific to each brine. However, the most accepted model is the weathering
58 of felsic rocks and/or local hydrothermal activity driven by a magmatic heat source through active
59 channel pathways (Bradley et al., 2013; Hofstra et al., 2013). In North America, several deposits have
60 been identified within the Basin and Range extensional province of the western United States,
61 including the Clayton Valley and the Great Salt Lake (e.g., Bradley et al., 2013). In South America
62 and more particularly on the Puna Plateau, brine deposits, referred to as *salars*, cover an area of about
63 400,000 km² from northern Argentina and northern Chile to western Bolivia (Ericksen and Salas,

64 1987) named the “lithium triangle”. In this area, several lithium deposits have been identified and are
65 operated by major mining companies including SCL/Chemetall and SQM/Tianqi Lithium Corp. In
66 China, the Qinghai-Tibet plateau is a favorable setting for lithium deposits, as illustrated by the
67 Qaidam (e.g., Shengsong, 1986; Yu et al., 2013) and Zabuye basins, from which some brines are
68 exploited by governmental mining companies.

69 *Hard-rock* deposits comprise several styles of Li mineralization in magmatic and/or
70 sedimentary rocks, related to both endogenous (magmatic) and exogenous (re-concentration by
71 weathering, or supergene alteration and transport) processes. They can contain widespread varieties of
72 Li-bearing minerals, such as Li-micas, Li-pyroxenes, Li-silicates, Li-phosphates, etc. (Table 1).
73 Among them, hectorite (Li-bearing clay) from the Kings Valley, Nevada (e.g., Glanzman et al., 1978;
74 Kesler et al., 2012) and jadarite (Li-bearing borosilicate) from Serbia (Stanley et al., 2007; Rio Tinto,
75 2017, Stojadinovic et al., 2017) represent potential world-class deposits, whereas spodumene-bearing
76 lithium-cesium-tantalum (LCT) pegmatites in the Greenbushes (Australia) have been mined for
77 decades by Talison Lithium Ltd. and others (e.g., Mudd and Jowitt, 2016).

78 Lithium production historically has been dominated by Australia (e.g., Greenbushes deposits),
79 South America (*Salar de Atacama*) and China (Zabuye, Qaidam Lakes). Thus, of the 36.5 kt Li metal
80 produced in 2016, 39% came from Australia, 32.8% from Chili, 15.6% from Argentina and 5.5% from
81 China. Portugal, the first Li producing European country, represents only 1.3% of world production,
82 especially for the ceramics and glass industry (BRGM, 2017). However, lithium exploration increased
83 significantly (e.g., Roskill Information Services Ltd., 2016), leading other countries in the European
84 Community (France, Austria, Czech Republic, Spain, Finland...) to assess their own mineral resources
85 and –reserves, in order to evaluate their global competitiveness in the lithium industry.

86 Hereafter, we provide a key to understanding the geological context of lithium in Europe from a
87 hard-rock perspective. To this end, we made a systematic, geographically- and geologically-based
88 compilation of lithium occurrences, significant mineral showings and/or deposits, with their
89 corresponding Li-deposit types, Li-bearing minerals and Li concentrations. For the first time, we
90 present an overview and quantification of identified European Li deposit types and features, and their
91 distribution in the different orogenic settings of Europe. A major effort was made to constrain
92 metallogenetically the Li endowments in order to highlight potential processes (endogenous and
93 exogenous) causing Li enrichment, and to introduce potential prospective regions. The resulting
94 dataset may be used in future studies for constraining the possible relationships between Li-rich
95 geothermal brines, surficial waters and Li-rich basement rocks.

96 2. Overview of hard-rock lithium deposit types in Europe

97 A compilation of lithium occurrences and -deposits was made by collecting information from various
98 geological survey organizations, exploration and mining companies, and scientific research projects
99 and related publications. This resulted in an up-to-date quantification of the European lithium
100 potential, considering only hard-rock ore types, identifying 527 lithium occurrences, projects and
101 deposits (provided as electronic supplementary material). This was almost five times more than the
102 previous Mineral4EU-ProMine (<http://minerals4eu.brgm-rec.fr/>) inventory (Cassard et al., 2015).

103 In addition, mineral resource and -reserve and -production data were gathered from available
104 published data by exploration and mining companies, such as technical and annual reports, from data
105 repositories (e.g., <https://sedar.com>) and from governmental surveys. Note that the data from England,
106 France and, locally, Germany are based on historical (before 1995), non-compliant CRIRSCO
107 (Committee for Mineral Reserves International Reporting Standards) compliant estimates.

108 We emphasize that lithium deposits related to seawater, and geothermal- and oilfield brines are not
109 considered in this study.

110 According to our compilation (and previous ones, e.g., Christmann et al., 2015), two distinct
111 categories of lithium deposits and occurrences are found in Europe. They are: 1) Magmatic-related
112 (Fig. 1A, B, C) deposits; and 2) Sedimentary/hydrothermal-related deposits (Fig. 1D).

113 2.1 Magmatic-related deposits

114 2.1.1 *Rare-metal granites*

115 Rare-metal granites (RMG; Černý et al., 2005) are felsic, peraluminous to peralkaline intrusive
116 rocks that host magmatic disseminated mineralization. They occur as very small, mostly subsurface,
117 granitic plugs, typically less than 1 km³, such as the Beauvoir RMG in France (Raimbault et al., 1995;
118 Fig. 1A). According to their geochemistry and geodynamic setting, three main types (Linnen and
119 Cuney, 2005; Černý et al., 2005) are recognized:

120 1) Peralkaline RMG have very high contents of F, REE, Y, Zr, Nb, related to anorogenic
121 settings; their Li content is relatively moderate (up to a few 1000 ppm) and is mainly illustrated by
122 zinnwaldite and polyolithionite occurrences (Tables 1, 2). This type is not documented in Europe;

123 2) Metaluminous to peraluminous, low- to intermediate-phosphorus RMG with high
124 concentrations of Nb, Ta, Sn, that occur in both post- and an-orogenic geodynamic settings. The Li
125 content again is moderate (up to a few 1000 ppm) and is mostly related to zinnwaldite. Examples
126 include Cinovec (Fig. 1C), Podlesi (Fig. 2A), the Sejby and Homolka granites in the Czech Republic,
127 the Chavence and Les Châtelliers granites in France (Table 2; Černý et al., 2005 and references
128 therein);

129 3) Peraluminous, high-phosphorus RMG with strong enrichment in Ta, Sn, Li and F, occurring
130 in a continental-collision setting. In this RMG type, Li concentrations can be high, from 0.5% to 1.0%
131 Li_2O , and occurring as lepidolite, Li-rich muscovite and amblygonite-montebbrasite series, such as at
132 Beauvoir (Figs. 1A, 2B), Montebbras (Fig. 2C) and the Richemont rhyolite dike in the French Massif
133 Central, and Argemela in Portugal (Table 2; Černý et al., 2005 and references therein).

134 2.1.2 LCT Pegmatites

135 With the exception of some rare giant Precambrian occurrences, lithium-cesium-tantalum (LCT)
136 pegmatites (e.g., London, 2008, 2018; Černý and Ercit, 2005) are relatively small-sized (a few m^3 to
137 $<1/2 \text{ km}^3$; Fig. 1B), coarse-grained and/or aplitic igneous rocks of granitic composition.
138 Geochemically, Li-rich LCT pegmatites are similar to peraluminous high-phosphorus RMG. They are
139 the result of crystallization of fluid-rich melts, enriched in various amounts of incompatible elements,
140 such as Li, Ta, Sn, Rb, Be, Nb and Cs, and strongly depleted in REEs, close to chondritic values
141 (London, 1995, 2005, 2008, 2018; Černý and Ercit, 2005; Černý et al., 2012; Linnen et al., 2012).

142 Pegmatites can form under various P/T conditions (Table 3) representing various classes (e.g.,
143 Černý, 1989, 1990; Černý et al., 2012). They are generally clustered in kilometer-size pegmatite fields
144 (e.g., the Ambazac pegmatite field, Deveaud et al., 2013; Silva et al., 2018), and occur as dikes and/or
145 sills (e.g., Emmes pegmatite, Finland, Eilu et al., 2012; Gonçalo pegmatite field, Portugal, Ramos et
146 al., 1994) or lenticular bodies (e.g., Bohemian pegmatites, Melleton et al., 2012). Contacts with host-
147 rock range from relatively sharp to progressive, depending on the nature of the host and the depth of
148 emplacement. Host-rocks are mainly metasedimentary and/or metavolcanic rocks metamorphosed
149 from lower greenschist to amphibolite facies (Černý, 1992) as well as granite intrusions (e.g.,
150 Gonçalo, Ambazac).

151 LCT pegmatites show heterogeneous textures and compositions, and are composed of variable
152 amounts of quartz, plagioclase, potassium feldspar, micas, with various amounts of garnet, tourmaline,
153 apatite and (usually) accessory Li-bearing minerals - locally rock-forming - such as spodumene,
154 petalite, etc. Although not systematically observed, LCT pegmatites generally show layering and/or
155 concentric zoning. Lithium-bearing minerals, including spodumene, petalite, the amblygonite-
156 montebbrasite group, lepidolite (Figs. 2D, E), eucryptite, elbaite and the lithiophilite-triophylite group
157 are commonly found in pegmatite bodies, whereas cookeite and holmquistite occur mainly in the
158 pegmatite aureole, or as secondary minerals (e.g., cookeite after petalite). Note that eucryptite may
159 reflect the alteration of primary spodumene. Li_2O content varies as a function of the LCT pegmatite
160 subtype and the Li-bearing minerals themselves (Table 3), ranging from 0.5 to 1.5%.

161 Mixed niobium–yttrium–fluorine (NYF)-LCT pegmatites are known from Norway (e.g.,
162 Birkeland, Frikstad, Skripeland) and Ukraine (Volodarsk-Volynsky). In Norway, pegmatite fields such
163 as Evje-Iveland show a typical initial NYF chemical signature, but are depleted in REEs and F in

164 replacement areas. Moreover, the replacement zones show a “cleavelandite signature” as well as
165 chemical and mineralogical LCT features, including beryl, columbite group minerals and tourmaline
166 (Černý, 1991a, b). Lithium-ore tonnages or grades are not reported for these pegmatites.

167 2.1.3 Greisen

168 Greisen deposits (e.g., St Austell, UK; Cinovec, CZ) result from a high-temperature hydrothermal
169 transformation of fractionated granitic intrusions (pegmatites, granites) with their upper part being a
170 porous muscovite-quartz assemblage at the granite/host-rock contact. They can occur as multi-stage
171 swarms crosscutting Sn-W quartz veins (e.g., Černý et al., 2005; Štemprok et al., 2005; Launay et al.,
172 2018), or may form up to 100-m thick units with irregular to sheet-like bodies. Li is mainly hosted in
173 micas, such as Li-rich muscovite, lepidolite, zinnwaldite, and amblygonite-montebbrasite group
174 minerals. Peraluminous RMG and metaluminous intrusions are favorable rock types for the
175 development of such deposit types (Fig. 1C), whereas fractionated granites appear to be unrelated with
176 significant Li endowment. Thus, the Li_2O content in the greisen around the world-class Panasqueira W
177 deposit (Portugal) is only about 732 ppm (Bussink, 1984), whereas Li_2O values from the Erzgebirge
178 province (e.g., Štemprok et al., 2005; Jarchovský, 2006) vary from 80 to 3100 ppm for greisen of the
179 RMG Vykmanov and Schnöd granites.

180 Quartz, cassiterite, wolframite, micas, topaz, tourmaline, sericite and chlorite are common in
181 greisen, showing vertical and horizontal zoning. Alteration is generally shown by kaolinization,
182 tourmalinization, feldspathization (microclinization and/or albitization) and greisenization forming
183 haloes around the granitic body. REE enrichment may occur and is indicated by precipitation of
184 monazite, xenotime and other REE-rich minerals.

185 Note that this deposit type can be related to both magmatic and hydrothermal processes. Here, we
186 consider a “granite-related” classification even though hot hydrothermal fluids are involved.

187 Co-products commonly consist of industrial minerals, such as feldspar, quartz and kaolin (e.g.,
188 Beauvoir, France); Sn and W are of first interest, Be, Ta, In, Sc, Rb representing potential byproducts.

189 2.1.4 Quartz-montebbrasite hydrothermal veins

190 Several authors (e.g., Martín-Izard et al., 1992; Roda-Robles et al., 2016) reported the existence of
191 quartz-montebbrasite hydrothermal veins associated with leucogranitic cupolas in the central part of the
192 Central Iberian Zone in Spain (e.g., Valdeflores, Barquilla, Golpejas, El Trasquilón) and Portugal
193 (e.g., Argemela area and Massueime).

194 Hosted by granites or metasedimentary rock of the Schist-Metagreywacke Complex, these
195 veins are generally <1 m thick and fill fracture sets. They contain a high proportion of quartz and few
196 minerals such as K-feldspars and micas (Roda-Robles et al., 2016). Accessory minerals such as Nb-Ta
197 oxides, cassiterite and sulfides are common, and Li-bearing minerals consist of the montebbrasite-

198 amblygonite series (Table 1). Note that only few Li_2O values are reported for these occurrences (i.e.,
199 0.45% Li_2O on average for the Argemela mine, PANNN, 2017) and, except for the Argemela mine,
200 such deposits appear to be relatively uneconomic in view of their small size.

201 *2.1.5 Tosudite mineralization related to gold deposits*

202 An occurrence of Li-bearing tosudite in the the Châtelet gold deposit (France) was reported in several
203 studies (Braux et al., 1993; Piantone et al., 1994); Li_2O values range from 142 to 920 ppm. These
204 authors suggested that the Li is related to late hydrothermal fluid circulation, itself related to the RMG
205 emplacement in the northern part of the French Massif Central.

206 *2.2 Sedimentary/hydrothermal/supergene deposits*

207 These types include deposits related to either sedimentary rocks affected (or not) by hydrothermal
208 processes, or surficial rocks affected by supergene weathering.

209 *2.2.1 Jadar deposit type*

210 In 2004, Rio Sava (a subsidiary of the Rio Tinto mining corporation) discovered the Jadar Basin in
211 Serbia, now considered as a “non-conventional” world-class lithium deposit through the occurrence of
212 the mineral jadarite (Stanley et al., 2007), a lithium boron silicate (Table 1). The basin consists of a
213 relatively large (>20 kilometers long) intramontane lacustrine (paleo)-evaporite basin composed of
214 dolomite, marble, various siliciclastic sedimentary rocks, pyroclastic units and notable oil shales
215 (Obradovic et al., 1997). The mineralization is hosted in a 400 to 500 m thick Miocene sedimentary
216 unit dominated by calcareous claystone, siltstone, sandstone and clastic rocks, unconformably
217 overlying a Cretaceous basement composed of various metasedimentary rocks, limestone, sandstone
218 and granite, including Miocene intrusions (Fig. 1D).

219 The lithium and borate mineralization occurs as 1.5 to 35 m thick stratiform lenses of three
220 gently dipping tabular zones covering a surface area of 3 by 2.5 km. The ore is composed of jadarite-
221 bearing siltstone and mudstone with locally interbedded sodium borate lenses (i.e., ezcurrite, kernite,
222 borax; Fig. 1D). Jadarite occurs as 1-10 mm white and rounded grains, nodules or concretions in the
223 siltstone or mudstone matrix that contains various amounts of calcite, dolomite, K-feldspar, rutile,
224 albite, pyrite, muscovite and ilmenite (Fig. 2F; Rio Tinto, 2017; Stanley et al., 2007). In 2017, the
225 mineral resources were reported as 135.7 Mt of ore at a grade of 1.86% Li_2O and 15.4% B_2O_3 (Rio
226 Tinto, 2017), representing a giant deposit of 2.524 Mt of Li_2O .

227 *2.2.2 Mn-(Fe) deposits*

228 Among the various types of host-rocks for Li-bearing minerals in Europe, the small-scale and
229 discontinuous Mn-Fe-rich sedimentary units (e.g., Drogol Mine in Scotland and Clews Gill in
230 England), exploited in the 19th century for their Fe and Mn contents, are a favorable site for secondary

231 Li-oxides such as lithiophorite (Table 1). Stratigraphically, they can be subdivided into two distinct
232 units: 1) a reddish siliciclastic host rock, mainly pelite, shale and/or sandstone, enhanced in Mn and Fe
233 relative to the average shale composition; and 2) discontinuous Mn lenses or layers (coticles). The
234 minerals include cryptomelane, goethite, hematite and other manganese oxides including Li-rich
235 lithiophorite, chalcophanite and pyrolusite.

236 The Li_2O content in lithiophorite is relatively low (1.23 wt.% for Li_2O versus 55 wt.% for
237 MnO), indicating an uneconomic lithium grade. However, its occurrence is relatively important in
238 view of the sedimentary and European histories (cf. Section 3 hereafter).

239 2.2.3 Bauxite deposits

240 Similar to the Mn-Fe deposit type, bauxite deposits can contain various amounts of lithiophorite,
241 cookeite (Table 1) and tosudite (Li-rich gibbsite; Nishiyama et al., 1975). Lithiophorite is the most
242 common Li-bearing manganese oxide mineral in karst bauxites. It occurs in several localities, such as
243 the Halimba, Fenyöfő and Kincsesbanya deposits in Hungary, where aluminum and gallium in bauxite
244 deposits were exploited from the 1950s to recently (Anderson, 2015).

245 Al and Mn are of first interest in this deposit type. The presence of lithiophorite and local
246 cookeite reflect Li enrichment, though this is not systematically evaluated. However, values of up to
247 0.53% Li_2O within bauxite are known from China (Wang et al., 2013) and the USA (Tourtelot and
248 Brenner-Tourtelot, 1977).

249 2.2.4 Other lithium deposit types

250 A few other deposit types show relatively minor anomalous lithium contents, including:

- 251 1) Mississippi-Valley type (MVT) deposits that include some lithiophorite (Usingen, Germany), and
- 252 2) Aalenian black shales from the Dauphinois region, Isère, France, where cookeite is disseminated in
253 black shale and in tension gashes crosscutting the shales (Jullien and Goffé, 1993). For the latter
254 occurrence, values (Henry et al., 1996) are in the range of 9 to 1 847 ppm Li_2O with an average of
255 441 ppm Li_2O (n=10). These lithium occurrences are symptomatic for local conditions allowing minor
256 enrichment, implying that they are not economically significant regarding their Li content.

257 2.3 Lithium resources and reserves

258 In Europe, lithium resources and reserves have been estimated or evaluated according to a CRIRSCO
259 (i.e., Committee for Mineral Reserves International Reporting Standards) reporting system, or based
260 on historical evaluations, for only 35 sites (Table 4). Thirteen occurrences in England, Ireland, France
261 and Germany, such as Beauvoir, Montebbras, St Austell or Aclare, were evaluated before systematic
262 reporting was established, and their mineral-resource and -reserve estimates are mostly based on
263 historic evaluations by geological survey organizations. Fifteen projects, including Jadar, are defined
264 in the Australian JORC classification; one project (Zinnwald) was defined in the European PERC; one

265 project (Alberta I) is defined in the Canadian NI43-101 system; Four projects in Ukraine are defined in
 266 an unknown system (Table 4); and one project is defined in the United Nations Framework
 267 Classification (UNFC). This list reflects the active exploration of lithium in Europe.

268 However, most of these deposits report mineral resources and only five specify reserve values,
 269 indicating that a feasibility study was carried out. This generally includes a study of potential
 270 processing and metallurgical-treatment methods, resulting in an economically feasible recovery of
 271 lithium from the various Li-bearing minerals.

272 In order to compare the Li-content in known Li-deposits, the sum of ore production + ore
 273 reserves + ore resources has been converted into contained Li_2O (ore tonnage x ore grade) for each
 274 deposit. These deposits were then categorized and classified into categories A, B, C, D and E¹
 275 according to their commodities and their reported mineral resources and -reserves (Table 4), following
 276 the system of the European ProMine database (Cassard et al., 2015). Note that we consider only the A,
 277 B, C and D categories as (potential) lithium deposits (Table 4), which corresponds to 28 deposits.

278 Among them, three deposits are identified as category A, including the Cinovec (Czech
 279 Republic), St Austell (UK) greisen and the Jadar deposit (Serbia). However, the historical estimate by
 280 the British Geological Survey for the St Austell deposit may be unrealistic, as it was based on
 281 extraction from an area of about 92.5 km² on the edges of protected landscape zones (British
 282 Geological Survey, 2016).

283 Lithium occurrences appear to be well distributed in Europe. However, the Iberian area and
 284 Finland regroup most of the identified lithium deposits (Table 4), indicating that these countries are
 285 relatively active in lithium exploration and suggesting that they have a strong Li-potential.

286 3. Lithium metallogeny in Europe throughout the Earth's evolution

287 In Europe, several orogenic events throughout geological history are associated with lithium
 288 mineralization. In this section, we assess and contextualize the lithium mineralization to orogenic
 289 features in order to establish—if possible—potential metallogenetic settings.

290 As a reminder, Europe's landmass results from a long geological history spanning 3.6 billion
 291 years, including the assemblage of numerous continental blocks. The European lithosphere can be
 292 broadly divided into two large regions: 1) The old East European Craton, partly covered by weakly
 293 deformed Phanerozoic and Meso- to Neo-Proterozoic rift and platform successions, mostly located in
 294 eastern and north-eastern Europe; and 2) A thinner, dominantly Phanerozoic, lithosphere, accreted to

¹ Category refers to: Category A $\geq 1,000,000$ t Li_2O ; $1,000,000$ t \geq Category B $\geq 100,000$ t Li_2O ; $100,000$ t \geq Category C $\geq 50,000$ t Li_2O ; $50,000$ t \geq Category D $\geq 5,000$ t Li_2O ; Category E $< 5,000$ t Li_2O , based on the sum of production + reserves + resources.

295 the East European Craton during Palaeozoic and younger orogenies, mostly in Western Europe (e.g.,
296 Gee et al., 2006; Artemieva and Thybo, 2013).

297 3.1 Hard-rock lithium mineralization in European Archean to Paleo-Proterozoic terranes

298 3.1.1 *The Ukrainian Shield (3.5 to 1.9 Ga)*

299 The Ukrainian Shield forms an assembly of Precambrian crystalline megablocks that is 900 km long
300 and 60-150 km wide in the central part of the country (Fig. 3A). This area is fault-bounded by the
301 younger Dnister-Fore Black Sea and the Dniprovsko-Donnetska metallogenic provinces, and was
302 affected by three distinct magmatic events at *ca.* 3.2, 2.6 and 1.9 Ga (Vinogradov and Tugarinov,
303 1961), which may have been partly coeval with the Svecofennian magmatism (2.1 to 1.8 Ga).

304 Several Li-rich deposits and occurrences are reported, such as: 1) the spodumene- and petalite-
305 subtype of lithium-cesium-tantalum (LCT) pegmatites that occur in the Dnester-Bug (Podolia) and
306 Azov Megablocks (e.g., Krutaya Balka, Nadyia); and 2) zinnwaldite and lepidolite occurrences in
307 mixed miarolitic niobium-yttrium-fluorine (NYF)-LCT pegmatites (e.g., Volodarsk-Volynsky) and
308 rare-metal granites (RMG), such as the Perzhanskoe ore district) in the Northern Volyn Megablock
309 (Kvasnista et al., 2016).

310 Although these lithium occurrences are known, only very little information is available. This
311 makes their evaluation, regarding metallogenic settings and geological context from a European
312 perspective, very difficult.

313 3.1.2 *The Svecofennian orogenic belt (2.1 to 1.8 Ga)*

314 The Svecofennian orogenic belt (Fig. 3) is part of the Columbia/Nuna supercontinent accretion that
315 took place from 2.1 to 1.8 Ga (Zhao et al., 2002). It consists of magmatic-arc accretionary phases
316 joining the juvenile Svecofennian arc terrane to the Archean Karelia Craton (Nironen, 1997) along the
317 Luleå–Kuopio thrust zone (Fig. 3; Zhao et al., 2002).

318 Prior to the Svecofennian orogen, continental break-up of the Karelian Province led to the
319 formation of an ocean basin and deposition of sedimentary units such as the 1.92 Ga Pohjanmaa schist
320 belt. Initial accretion started at 1.91 Ga and ended at 1.87 Ga, followed by large-scale extension in a
321 back-arc setting (1.87-1.84 Ga) shown by psammites/pelites and intruded by granites and mafic dikes
322 (Korja et al., 2006). An oblique continent-continent collision occurred from 1.87 to 1.79 Ga, illustrated
323 by the advancing accretion of retro-arc fold-and-thrust belts with alkaline bimodal magmatism (e.g.,
324 Lahtinen et al., 2009). Significant lithospheric thickening, local migmatization and formation of S-type
325 granites in southern Finland and central Sweden occurred as well. Finally, gravitational collapse ended
326 the orogen between 1.79 and 1.77 Ga. Two major amphibolite grade metamorphic events are recorded
327 at 1.88-1.87 Ga (Lecomte et al., 2014) and 1.83 to 1.80 Ga (Eilu et al., 2012).

328 Within this geological framework, lithium mineralization took place in metasedimentary and
329 metavolcanic units along major fault and shear zones. They are dated as relatively late, between 1.8 to
330 1.79 Ga (Fig. 3, Table 5; e.g., Alviola et al., 2001), post-dating local migmatization. They include the
331 *ca.* 1.88-1.86 Ga Vaasa Migmatite Complex on the margins of the Evijärvi belt (Suikkanen et al.,
332 2014), and the *ca.* 1.84-1.82 Ga late-orogenic migmatizing microcline granites in southwestern
333 Finland (Kuhila et al., 2005), and appear coeval with the regional amphibolite-grade metamorphism.
334 The mineralization occurs as LCT pegmatite fields, such as the Kaustinene and Somero-Tammela
335 fields (Fig. 3). The Kaustinene one occurs in the 1.92 Ga Pohjanmaa schist belt comprising the Länttä,
336 Syväjärvi and Outovesi deposits, which are albite-spodumene pegmatites owned by Keliber Oy. In the
337 Somero-Tammela region (Fig. 3), the petalite/spodumene Luolamaki, Hirvikallio and Kietyömaäki
338 LCT pegmatites, owned by Nortec Minerals Corp., are hosted in the Håme belt that consists of
339 metavolcanic rock intercalated with metagreywacke and metapelite. In these pegmatites, petalite was
340 formed first and later converted to spodumene, suggesting a temperature decrease at constant pressure
341 during crystallization that involved rapid cooling of the terranes (Eilu et al., 2012). Triphylite is
342 reported from several LCT pegmatites, mainly in Sweden.

343 3.1.3 The Sveconorwegian orogenic belt (1140 to 850 Ma)

344 Part of the Grenvillian orogeny, the Sveconorwegian orogenic belt is related to the collision between
345 Fennoscandia and an undetermined major plate (likely Amazonia), which contributed to the Rodinia
346 supercontinent assembly (e.g., Li et al., 2008). The orogen spans from 1140 to 850 Ma, amalgamating
347 Mesoproterozoic (1750-1500 Ma) lithotectonic units separated by major shear zones (Bingen et al.,
348 2008a, b); according to these authors, the orogen can be divided into several tectonic phases. Among
349 these, the Arendal phase (1140-1080 Ma) marks the collision between the Idefjorden and Telemarkia
350 terranes (Fig. 3). This initial phase was related to closure of an oceanic basin, and subsequent accretion
351 of a volcanic arc and a high-grade metamorphic event (*ca.* 1140-1125 Ma). The Adger phase (1050-
352 980 Ma) corresponded to oblique continent-continent collision, and underthrusting and
353 burial/exhumation of the Idefjorden Terrane (Fig. 3). This phase was contemporaneous with crustal
354 thickening of the Telemarkia Terrane, when widespread syn-collisional magmatism was followed by
355 high-grade metamorphism. Finally, the Dalane phase (970-900 Ma) corresponded to gravitational
356 collapse, associated with post-collisional magmatism, and formation of a gneiss dome and core
357 complex (930-920 Ma) with low-pressure/high-temperature metamorphism.

358 In this context, lithium mineralization occurred within polymetamorphic Paleoproterozoic
359 amphibolite gneiss, gabbroic amphibolite and metadiorite, mainly within the Idefjorden and Telemark
360 terranes. In the latter, the Evje-Iveland pegmatite field, recognized as the largest one (Fig. 3; e.g.,
361 Birkeland and Frikstad), comprises over 400 pegmatite bodies. These were dated at *ca.* 909±14 Ma
362 (Scherer et al., 2001; Table 5), appear to be unrelated to granites, but are coeval with late regional

363 partial melting and crustal collapse. Among these NYF pegmatites, several indicate a late-magmatic
364 event shown by a REE-depleted replacement zone consisting of “cleavelandite”, amazonite, quartz and
365 muscovite, suggesting overprinting of a LCT magma onto pre-existing NYF pegmatite bodies (Černý,
366 1991a,b). Lepidolite and zinnwaldite are reported from these pegmatites, which are considered as
367 mixed NYF-LCT pegmatites, although the Li enrichment is related to the replacement zones.

368 3.2 Hard-rock lithium mineralization in European Neoproterozoic to Neogene terranes

369 3.2.1 *The Cadomian orogenic belt (620-540 Ma)*

370 In Europe, the Cadomian orogeny is characterized by a continental magmatic arc, which occurred
371 during the Ediacaran along the rim of the West African Craton and resulted in opening of the Rheic
372 Ocean between the Avalonia and Armorica microplates, respectively associated with the Laurentia and
373 Gondwana supercontinents. This took place from Cambrian to Ordovician (Fig. 4; e.g., Linnemann et
374 al., 2008; Nance et al., 2012).

375 A notable relic of this event is the occurrence of discontinuous Cambrian-Early Ordovician
376 Mn-(Fe) rich metasedimentary rocks in Scotland, Wales, the Lake District of England, Belgium and
377 Germany (Fig. 4; Kroner and Romer, 2013). Here, Li-bearing minerals such as lithiophorite can occur.
378 Such occurrences are restricted to the Avalonian Shelf, constrained by the Rheic suture in the south,
379 and were formed by weathering of the Cadomian continental magmatic arc at the edge of the peri-
380 Gondwana plate in an extensional regime (Romer et al., 2011). They were formed during the first
381 stage of the orogeny (*ca.* 590-570 Ma) and are not stratigraphically correlative, but can be found along
382 the Avalonia Shelf from Nova Scotia through the Government Point Formation of the sedimentary
383 Goldenville Group (Canada; White, 2008) to Poland. Kroner and Romer (2013) suggested that coeval
384 and similar deposits may be found in the southern part of the Ossa Morena Zone (Spain).

385 3.2.2 *The Caledonian orogenic belt (475-380 Ma)*

386 The Caledonian orogeny was a series of tectonic events related to the closure of the Iapetus Ocean
387 (McKerrow et al., 2000), reflecting Ordovician-Silurian oblique interactions between the Laurentian
388 (Scotland), Avalonia (Ireland) and Baltica terranes. The initial Grampian phase (475-460 Ma)
389 consisted, at the north end of the Iapetus Ocean, of collision between the Laurentian continental
390 margin and an intra-ocean island arc complex. This resulted in the emplacement of S-type granites in
391 the NW highlands of Scotland and was followed by oblique subduction under the Laurentian (north),
392 Avalonian (south) and Baltica (east) terranes (Fig. 5A). In the Late Silurian (425 Ma), the Iapetus
393 Ocean was closed and continents collided with the Laurentian Terrane along the Iapetus Suture Zone
394 (Fig. 5A). Widespread calc-alkaline magmatism occurred from *ca.* 425 to 380 Ma as a post-subduction
395 event (Miles et al., 2016), related to orogen-wide sinistral transtension induced by subsequent episodes
396 of lithospheric extension during the Early Devonian (Brown et al. 2008).

397 In this Caledonian context, LCT pegmatites are known from Scotland and Ireland. In Scotland,
398 the Glenbuchat pegmatite lies in the northern part of the Iapetus Suture Zone, hosted by Dalradian
399 metasedimentary rocks of the Grampian Terrane. It consists of lepidolite and elbaite rich pegmatite
400 (Fig. 5B; Jackson, 1982). The Dalradian Inzie Head gneiss and Grampian granite are associated with
401 the *ca.* 470 Ma Grampian migmatization (Johnson et al., 2001).

402 In Ireland, the *ca.* 412 Ma Leinster LCT pegmatite field (Table 5; Barros, 2017) that includes
403 the spodumene Aclare and Molyisha pegmatites, shows a relatively late time of formation (Fig. 5B).
404 The pegmatite field is hosted by the *ca.* 417-405 Ma poly-phase Tullow Lowlands pluton (Fritschle,
405 2016) along the East Carlow Deformation Zone and includes up to 60 wt.% spodumene (Luecke,
406 1981). Thus, their emplacement may be related to a transtensional regime in this late orogenic process.

407 3.2.3 The Variscan orogenic belt (400-250 Ma)

408 The European Variscan orogen extends from southern Iberia to northeastern Bohemia, forming a
409 3000 km long and 700-800 km wide belt. It results of Late Paleozoic convergence and collision of the
410 Gondwana (south) and Laurasia-Baltica (north) megacontinents along the Variscan Front (Fig. 6),
411 involving several intermediate microcontinents and closures of oceanic domains (e.g., Matte, 1986,
412 1991).

413 The earliest continental collision started locally in the Early Devonian (385-380 Ma) with
414 migmatization and related anatexis of continental crust, as well as exhumation of Late Silurian rocks
415 along a regional deformation event. In the Middle-Late Devonian (360-350 Ma), arc and back-arc
416 magmatism occurred in the northern Gondwana margins and Central Armorican Domain, attesting of
417 southward subduction and subsequent closure of the Rheic Ocean (Fig. 6; Faure et al., 2005). This
418 event was associated with a variable pressure-temperature metamorphic and deformation event. Late
419 Viséan synorogenic extension related to a synorogenic collapse of the inner zones occurred along NW-
420 SE stretching and 333 to 326 Ma migmatization (Faure et al., 2005). Finally, post-orogenic collapse
421 took place around 300 Ma. It was coeval with N-S extension, development of intramontane coal basins
422 and *ca.* 306 Ma local migmatization (Faure et al., 2005). These events appear to have been
423 diachronous throughout the Variscan orogeny.

424 Considerable amounts of granitic intrusions and several districts of RMG/greisen and LCT
425 pegmatite deposits illustrate the Variscan orogeny. At the scale of the belt, such deposit types are
426 relatively late in the orogeny, coeval with crustal extension together with regional partial melting and
427 melt emplacement. Thus, in the Bohemian Massif, the easternmost part of the European Variscan belt
428 (Fig. 6), greisen and RMG are common in the Saxothuringian and Teplá-Barrandian zones consisting
429 of Neoproterozoic basement (e.g., Matte et al., 1991). The Moldanubian area contains mainly LCT
430 pegmatites (e.g., Cháb et al. 2010, Ackerman et al., 2017), which appear to be spatially related to
431 migmatitic domes and shear zones. According to Melleton et al. (2012), two ages of pegmatite

432 emplacement were identified, including an independent orogenic stage in the Bohemian Massif with
433 LP-HT regional metamorphism related to significant reheating and anatexis; they note that the
434 emplacement of LCT pegmatite here is the oldest known magmatic event of the Variscan orogeny.

435 In France, the northwestern part of the Massif Central is a favorable area for rare-element
436 magmatic bodies (Marignac and Cuney, 1999). This province can be divided into three distinct deposit
437 types (Table 5): 1) rare-metal granite such as the 317 ± 6 Ma Beauvoir and the 314 ± 4 Ma Montebbras
438 (Aubert, 1969; Cuney et al., 1992, 2002); 2) rare-metal rhyolite represented by the 313 ± 3 Ma
439 Richemont rhyolite (Raimbault and Burnol, 1998); and 3) LCT pegmatites such as the Mont
440 d'Ambazac rare-element pegmatite field (e.g., Raimbault et al., 1995; Deveaud et al., 2013). The latter
441 includes the 309 ± 5 Ma lepidolite-subtype LCT Chédeville pegmatite, which postdates the 324 ± 4 Ma
442 host granite (Hollinger et al., 1986) and appears to be sub-synchronous with local partial melting
443 (315 ± 4 and 316 ± 4 Ma; Gébelin et al., 2009) and with shearing (La Marche shear zone: 316 ± 5 to
444 312 ± 2 Ma, Gébelin et al., 2007, 2009). This east-west La Marche fault system, located in the northern
445 part of the Limousin, appears to have been a key-control on magmatic activity (Cuney et al., 2002).

446 The Galicia-Trás-os-Montes Zone (GTOMZ) and the Central Iberian Zone (CIZ) in the Iberian
447 Variscan belt host widespread LCT pegmatite fields. At least five main mineralized pegmatite fields
448 are recognized in the former from north to south: Forcarei-Lalín, Serra de Arga, Barroso- Alvão, La
449 Fregeneda-Almendra and Gonçalo-Guarda. In the CIZ, the 326 ± 3 Ma Argemela granite is the only
450 RMG known from Iberia (Charoy and Noronha 1991; 1996). The average age of intrusion of LCT
451 pegmatites in the GTOMZ is 310 ± 5 Ma, whereas in the CIZ and in the southern GTOMZ the ages are
452 younger: 301 ± 3 Ma (Melleton et al., 2011), 295.1 ± 4.1 Ma and 296.4 ± 4.1 Ma (Roda-Robles et al.,
453 2009; Vieira, 2010). Moreover, late quartz-montebbrasite hydrothermal veins are reported from several
454 areas in the CIZ (e.g., Roda-Robles et al., 2016).

455 Finally, in the Austroalpine unit of the Eastern Alps, Permian LCT spodumene-bearing pegmatites
456 are known (e.g., Thöni and Miller, 2000; Ilickovic et al., 2017). These pegmatites appear to be coeval
457 with lithospheric extension, causing crustal basaltic underplating, HT and LP metamorphism, as well
458 as intense magmatic activity (Schuster and Stüwe, 2008).

459 3.2.4 *The Mediterranean and circum-Mediterranean orogens (Mesozoic-2.5 Ma)*

460 Several styles of lithium mineralization are contemporaneous with the circum-Mediterranean and
461 Mediterranean Tethys mountain belts, such as the Carpathians Mountains or the Egean Domain, which
462 resulted from oceanic closure and collision of the European continental foreland (Bohemian Massif)
463 with the African promontory of the Adriatic microplate (Fig. 7). Rifting of the Alpine Tethys and its
464 subsequent subduction underneath the Adriatic margin, followed by continent-continent collision,
465 promoted widespread magmatic activity through time, as well as the development of related orogens
466 such as the Carpathians Mountains.

467 The initial continental rifting of the Alpine Tethys and its related magmatism occurred from the
468 Middle to Late Triassic in the eastern part of the Mediterranean domain (Bertotti et al., 1999; Schmid
469 et al., 2008). In the central Alpine-Carpathian-Dinaridic orogenic system, *ca.* 242 Ma Li-phosphate
470 pegmatites occur in the Brissago area (Switzerland; Vignola et al., 2008); these authors suggested that
471 the pegmatites formed from partial melting of the Early Permian Ivrea gabbro.

472 This tectono-magmatic event was followed by development of the Adriatic passive margin in the
473 Middle Jurassic (Bertotti et al., 1999; Schmid et al., 2008) in an extensional tectonic regime, and later
474 by the subduction of the Tethys oceanic lithosphere beneath the Adriatic margin from Cretaceous to
475 Late Paleogene. This crustal shortening led to the final consumption of the Neotethys Ocean
476 associated with widespread calc-alkaline magmatism in the Carpathian arc (Fig. 7; Schmid et al.,
477 2008) and formation of the Apennines in Italy. Meanwhile, Jurassic to Cretaceous bauxite deposits
478 with lithiophorite are reported from Hungary and Greece (Fig. 7), suggesting a tropical climate during
479 this period.

480 In the external domain of the Dauphinois zone (French Alps), an Eocene greenschist metamorphic
481 event led to the formation of cookeite-bearing formations and -tension gashes within Aalenian black
482 shales (Fig. 7). According to Jullien and Goffé (1993), the Li was sourced from the metasediments that
483 themselves resulted from erosion of the continental crust.

484 Within the Central Alps (i.e., Penninic Zone), a kilometer-scale east-west extensional area occurs
485 with several Oligocene-Miocene LCT pegmatites in the Vigizzo, Bodengo and Codera areas. They are
486 Tertiary (Fig. 7; 30 to 20 Ma, Guastoni et al., 2014; Romer et al., 1996) and show a beryl-phosphate
487 affinity with elbaite and columbite as potential accessory minerals (Guastoni et al., 2014, 2016).

488 Finally, extensional collapse and back-arc extension promoted development of the Miocene
489 Pannonian and the Jadar basins within the Alpine-Carpathian-Dinarides domain along several late
490 Oligocene–Miocene detachment zones (Jolivet et al., 2009; Menant et al., 2018; Stojadinovic et al.,
491 2017) and in response to rapid slab roll-back (Simić et al., 2017; Stojadinovic et al., 2017). Basin
492 formation was accompanied by calc-alkaline magmatism with a paroxysm of silicic volcanism during
493 the early and middle Miocene (Kovács et al., 2007). Rapid exhumation of metamorphic rocks caused
494 episodic migmatization as well as related magmatism (Bergell intrusion; Beltrando et al., 2010).

495 Within the northern part of the Apennines, the *ca.* 6.7–6.9 Ma (Ferrara and Tonarini, 1985) LCT
496 pegmatites from Elba Island are famous for their gem-quality elbaites.

497

498 **4. Interpretation and discussion**

499 Considering all lithium occurrences in Europe, one of the first observations regarding their distribution
500 is their apparent clustering (Figs. 3, 4, 5, 6, 7). This clustering defines pegmatite and/or RMG fields
501 with similar ages of emplacement, suggesting a relatively coeval magmatic activity related to common
502 endogenous processes. Furthermore, the Li-rich sedimentary basins such as Jadar reflect late
503 sedimentary/hydrothermal Li re-concentration through exogenous processes. [Endogenous processes](#)
504 [related to lithium mineralization](#)

505 We have identified several Li-magmatic events through time as illustrated by RMG, greisen and LCT
506 pegmatites (Table 5; Figs. 3, 4, 5, 6, 7, 8), ranging from Paleoproterozoic to Miocene. These events
507 occurred during times of collisional orogeny, including the Svecofennian (2.1-1.8 Ga; Fig. 3),
508 Sveconorwegian (1140-850 Ma; Fig. 3), Caledonian (490-390 Ma; Fig. 5), Variscan (400-250 Ma;
509 Fig. 6) and Mediterranean (Mesozoic-2.5 Ma; Fig. 7) orogenies. These events were mainly related to
510 supercontinent formation, as observed elsewhere by Bradley (2011). Accordingly, in the Svecofennian
511 orogen, LCT pegmatite ages are 1.8-1.79 Ga This suggests relatively late emplacement in the orogenic
512 cycle that postdated arc accretion and the first regional metamorphism, and might be related to crustal
513 thickening as well as to a late amphibolite-facies metamorphic event.

514 During the Sveconorwegian orogen, emplacement of Li-rich pegmatites (910-906 Ma) appears
515 coeval with the late Dalane phase (970-900 Ma), corresponding to gravitational collapse and post-
516 collisional magmatism, as well as the formation of a gneiss dome and core complex related to low
517 pressure/high temperature metamorphism. The Scottish and *ca.* 412 Ma LCT pegmatites from Ireland,
518 which are part of the Caledonian orogenic belt, appear coeval with crustal thickening and post-
519 subduction magmatism.

520 In the Variscan belt, RMG (Beauvoir, Montebas and Richemon, France; Argemela, Portugal;
521 St Austell, UK), greisen (Cligga Head, Tregonning-Godolphin, Meldon, UK; Dlha Dolina, Slovakia;
522 Montebas, France; Krasno-Konik, Krupka, Czech Republic) and various LCT pegmatites (Table 5,
523 Fig. 6) are widely distributed (Fig. 8). Their ages suggest mostly emplacement during the Late
524 Carboniferous (Table 5) reflecting highly fractionated magmatic events throughout the European core
525 related to a post-collisional stage ending the Variscan orogeny *sensu stricto* (Fig. 6, Table 5; e.g.,
526 Bonin, 1998; Chen et al., 1993; Cuney et al., 2002; Melleton et al., 2012; Neace et al., 2016).
527 Moreover, from the internal to the external orogenic domains Li-magmatism appears to be
528 diachronous, indicating southward prograding Li-rich magmatic activity traversing the entire belt. In
529 the internal zones (France, Germany, Czech Republic and NW Iberia) RMG, greisen and LCT
530 pegmatites were mostly emplaced between 320 and 307 Ma corresponding to the Bavarian phase (330-
531 315 Ma; Finger et al., 2007) in the Bohemian Massif and to synorogenic collapse and NW-NE
532 stretching in the French Massif Central (320-310 Ma). In the external zones (UK, parts of Spain and

533 Portugal), similar deposits tended to be emplaced around 305 and 301 Ma (excluding the *ca.* 326 Ma
534 Argemela granite) suggesting late-orogenic magmatism (Melleton et al., 2015). Finally, deposits
535 belonging to the Gemeric unit in the Western Carpathians of Slovakia, as well as the Austroalpine
536 pegmatites of the Eastern Alps that form the extreme margins of the belt, indicate Permian ages coeval
537 with regional partial melting (Finger et al., 2003, Petrik et al., 2014; Ilickovic et al., 2017).

538 Thus, it appears that the emplacement of RMG, greisen and LCT pegmatites was relatively late in
539 the orogenic cycle and may have been coeval with continent-continent collision, commonly postdating
540 arc accretion. It could also be related to crustal thickening (Alviola et al., 2001), a favorable setting for
541 crustal peraluminous melt (Cuney et al., 1992; 2002) through wall-rock assimilation, the unmixing of
542 restite, and/or internal fluid circulation related to convective fractionation (Lehmann, 1994; Martin and
543 De Vito, 2005).

544 Importantly, it also appears that the reported greisen were developed from RMG, suggesting that
545 most of the greisen associated with fractionated S-type peraluminous granite may not show significant
546 Li contents. The formation model involves early exsolution of an F-CO₂-H₂O-rich aqueous phase from
547 the granitic magma, along with fluid/rock interactions leading to dissolution/precipitation and re-
548 concentration of incompatible elements, such as Li, F, Sn, W, etc., within the greisen (Heinrich, 1990).
549 Here: 1) miarolitic cavities are common and reflect volatile saturation; and 2) a decrease in rock
550 volume and increase of porosity are reported. In the 321.5±3 Ma Cinovec deposit, dissolution of the
551 protolithionite—formed during magmatic intrusion—and precipitation of zinnwaldite during
552 greisenization have led to remobilization of Li into its final host mineral (Johan and Johan, 2005).

553 4.2 Exogenous processes related to lithium occurrences

554 Several Li-occurrences in Europe reflect a concentration of lithium in sedimentary rocks through
555 various exogenous processes, such as hydrothermal circulation and/or erosion and transport. Thus,
556 distinct occurrence types can be distinguished.

557 4.2.1 *Jadar deposit type*

558 The Jadar deposit type is exclusively Neogene (Oligocene to Pliocene), based on available data. The
559 existence of several other isolated intramontane lacustrine evaporite basins is suggested in Serbia
560 (Fig. 8) as well as in Bosnia, such as the Valjevo-Mionica or Lopare basins from where jadarite was
561 reported. Interestingly, the subsurface of these basins includes LCT pegmatite and Cretaceous to
562 Miocene granitic intrusions, suggesting local lithium enrichment in the basement (Stojadinovic et al.,
563 2017). These basins were formed during the late stage of the Dinadric orogeny (Fig. 7), coeval with
564 the extensional collapse and back-arc extension due to Carpathian slab retreat (Simić et al., 2017).

565 Jadarite precipitation is poorly constrained. Some authors suggested that interaction between
566 clastic sedimentary rocks and the surrounding brine—possibly involving hydrothermal devitrification

567 and hydration of andesitic-dacitic pyroclastic material or alteration of clay minerals—may contribute
568 to its precipitation (Stanley et al., 2007; Stojadinovic et al., 2017).

569 *4.2.2 Mn-(Fe) deposits*

570 Two distinct periods of Mn-(Fe) precipitation in Europe are described here. A first group of deposits
571 in Scotland, Wales (e.g., Drosgol Mine), England (Clews Gill), Belgium (Otré, Beez) and Germany
572 (Harz) is Cambrian to Early Ordovician in age (Fig. 8; Waldron et al., 2011; Romer et al., 2011),
573 representing a notable relic of the Cadomian orogeny (650-550 Ma; Fig. 4). They are exclusively
574 located in the Avalonian plate, constrained by the Rheic Suture, and are formed from weathering of
575 the Cadomian magmatic arc of the Gondwana plate, as suggested by Nd and Sr isotopes (Romer et al.,
576 2011). Interestingly, in Europe, the Cadomian orogeny was subsequently reworked during the
577 Caledonian and Variscan orogenies (Zelazniewicz et al., 1997; Melleton et al., 2012).

578 The second group is mainly found in Hungary, where the Eplény and Urkut Mn deposits are
579 Jurassic in age (Polgari et al., 2005; Figs. 7, 8). These deposits are associated with marine sedimentary
580 rocks mainly composed of bioclastic limestone and black shale.

581 The Li-bearing mineral lithiophorite, as most Mn- and Fe-oxides, was formed from secondary
582 fluid circulation in the host rock (Nicholson and Anderton, 1989). Romer et al. (2011) suggested that
583 the lithium component derived from chemical weathering of continental crust and was originally
584 concentrated in siliciclastic or carbonate rocks. Thus, late hydrothermal fluid circulation may have
585 remobilized—and still remobilizes—the Li₂O content via dissolution/precipitation processes, thus
586 helping the precipitation of Li-bearing oxides under oxidizing conditions. Moreover, several authors
587 pointed out their distribution along regional faults that are favorable sites for fluid circulation, such as
588 the Candwr Fault in Wales (Cotterell et al., 2009) and the Red Gill Fault in the UK (Clark, 1963).

589 *4.2.3 Bauxite deposits*

590 Li-bearing minerals in bauxite deposits are Cretaceous in Hungary (D'argenio and Mindszenty, 1986)
591 and Jurassic to Cretaceous in Greece where they are located along the northern shores of the
592 Mediterranean Sea (Bardossy, 1982).

593 In Hungary, these deposits are stratiform where bedrock is a non-uniform karst carbonate rock,
594 in which the bauxite horizons are relatively large. The Halimba mining district is one of the largest,
595 with bauxite thickness varying from 1 to 40 m. Here, the Li-bearing mineral lithiophorite originated
596 from secondary fluid circulation through the host rock (Bardossy, 1982) forming Mn-rich layers in
597 epi- and supergene crusts. Cookeite is also reported from these deposits (Bardossy, 1982).

598 4.3 Discussion of rare-metal magma formation

599 There are currently two distinct models of rare-metal magma formation. The first one involves the
600 escape of late-stage melts ending the crystallization of huge highly fractionated felsic magma
601 chambers (e.g., Jahns and Burnham, 1969; London, 1992). One of the major arguments for this model
602 is the regional zoning of pegmatite bodies in the margins of supposed parent granites (e.g., Cameron et
603 al., 1949; Černý et al., 2005). An example is the Fregeneda-Almendra pegmatite field where crystal-
604 fractionation modelling and geochronology support a magmatic origin (Vieira 2011; Roda-Robles et
605 al., 2016). Moreover, the widespread presence of pegmatites and RMG in granites (e.g., London,
606 1992; Černý et al., 2005) suggests a granite-related origin (e.g. Roda-Robles et al., 2016).

607 However, some aspects disagree with this model, suggesting a second model that involves low-
608 grade partial melting of crustal sequences (e.g., Norton, 1973; Zasedatelev, 1977; Stewart, 1978;
609 Melleton et al., 2011; Müller et al., 2015; Bongiolo et al., 2016). In southern Ireland, geochemical
610 evidence points to the absence of a relationship between the LCT-spodumene Aclare pegmatite field
611 and the surrounding Tullow Lowlands and Blackstairs plutons that are part of the Leinster Granite.
612 This absence concerns their capacity of generating a residual pegmatite melt (Barros et al., 2016).
613 These authors suggested a separate partial-melting event for both units, although the intrusion of the
614 granitic unit may have triggered anatexis of the surrounding sedimentary rocks.

615 In the French Massif Central, the Monts d'Ambazac pegmatite field has $\delta^7\text{Li}$ mica values that are
616 consistent with a crustal metasedimentary source. It is also coeval with evidence of a partial-melting
617 event, excluding the influence of magmatic fractionation from the nearby St Sylvestre granite in the
618 formation of pegmatites. It also demonstrates that strong Li enrichment in pegmatite is not related to a
619 fractionation process (Deveaud et al., 2015). In the Bohemian Massif and in Austria, LCT pegmatite
620 fields are also supposed to be formed by partial melting processes (Melleton et al., 2012).

621 Thus, a model of partial melting during anatexis of sedimentary rock (evaporites, cookeite-bearing
622 metapelite, Li-rich metasedimentary rock, or Li-rich Ordovician orthogneiss, etc.) may be applied
623 (Fig. 10), involving coeval emplacement for S-type granite (e.g., Kontak et al., 2002) and nearby LCT
624 pegmatite, but not promoting a “parental” relationship. Moreover, micas, garnet and staurolite, which
625 are widespread in metasedimentary rock, are seen as a potential source for lithophile elements such as
626 Li (London, 2005, 2018). For instance, in the Brissago-Valle di Ponte area (Switzerland-Italy), poorly
627 fractionated LCT phosphate pegmatites are suspected to be derived from local partial melting of
628 kinzigites during high-temperature metamorphism (Vignola et al., 2008). At the European scale,
629 various Li-bearing minerals are reported from pegmatites, including Li-micas, lepidolite, spodumene
630 and petalite, involving variations in the fluxing content (F, B and P) of the magmatic fluid (Roda-
631 Robles et al., 2010), as well as varying P/T conditions (e.g., spodumene versus petalite; London, 1986,
632 1990). These variations are also seen in the Scandinavian orogenies, where zonation of Li-bearing

633 minerals is highlighted: 1) the Svecofennian LCT pegmatites are associated with Li-silicate and Li-
634 phosphate minerals; but 2) the Sveconorwegian LCT pegmatites show a Li-phyllsilicate affinity.

635 **4.4 From source to sink**

636 As suggested above, several parameters may control the lithium mineralization locations in Europe.
637 The observed clustering of endogenous lithium deposits such as LCT pegmatites, RMG and/or greisen
638 may involve a crustal anomaly (>20 ppm; Rudnick and Gao, 2004), or a Li “pre-concentration” related
639 to paleoenvironmental sedimentation conditions (e.g., type of basin, host rock, climate) and/or post-
640 deposition processes (weathering, basin-fluid circulation in the crust), more generally preserved along
641 a paleo passive-margin (Fig. 9; Romer and Kroner, 2015).

642 In any case, this involves the existence of a primary Li-source that can be of magmatic origin,
643 such as erosional material from a continental magmatic arc and related Mn(-Fe) deposits and
644 lithiophorite occurrences. Another possibility is a sedimentary origin, such as the Schist-
645 Metagreywacke Complex in the Galicia-Trás-Os-Montes Zone (Roda-Robles et al., 2016), or the
646 Pohjanmaa schist belt in Finland and related LCT pegmatites (Eilu et al., 2012). In that respect,
647 significant lithospheric thickening may be favorable for concentrating Li in a specific location (Eilu et
648 al., 2012). The occurrence of several types of Li mineralization in the French Massif Central (Fig. 6;
649 LCT pegmatite, greisen, RMG, Li-bearing tosudite) forming clusters may suggest a possible common
650 Li-source (Cuney and Barbey, 2014). Moreover, a recent isotopic $\delta^7\text{Li}$ study of pegmatites (Deveaud,
651 2015; Deveaud et al., 2015), suggested that beryl-columbite and lepidolite-petalite LCT pegmatites
652 from the Monts d'Ambazac show a distinct crustal contribution, indicating that Li-rich sources may
653 contribute to “secondary” lithium deposits if suitable processes are involved.

654 The timing of fluid circulation appears to be another important feature for Li-concentration,
655 whether related to a regional or to a local extensional regime in an orogenic cycle (Figs. 9, 10; e.g.,
656 Eilu et al., 2012; Jolivet et al., 2009; Melleton et al., 2015; Stojadinovic et al., 2017; Menant et al.,
657 2018). Sedimentary/hydrothermal lithium deposits are thus mainly related to regional extension
658 (rifting or back-arc extension; Kroner and Romer, 2013; Simić et al., 2017; Stojadinovic et al., 2017),
659 whereas magmatic-related lithium deposits are associated with local decompression and/or
660 transtension strike-slip deformation in late continent-continent orogenic cycles, leading to the
661 formation of a volatile-rich melt (Fig. 10). According to Kontak et al. (2002), this melt may cause
662 over-pressuring and/or hydro-fracturing, resulting in the formation of dilatant zones and related
663 fracture sets. Remarkably, sedimentary rocks enriched in Li during an extensional regime (e.g., Jadar
664 Basin) may be a favorable Li source during a subsequent magmatic event. Unfortunately, a lack of
665 data makes it impossible to confirm this hypothesis.

666 Finally, the distribution of Li-occurrences is strongly influenced by the location and geometry of
667 fracture sets (Figs. 9, 10; Deveaud et al., 2012; Deveaud, 2015; Silva et al., 2018). High permeability

668 fractured zones seem to act as favorable channels for: 1) The emplacement of LCT pegmatite or RMG
669 from evolved magma; or 2) Hydrothermal fluid circulation through sedimentary successions (Jadar
670 Basin, lithiophorite occurrences in Aalenian black shales) leading to secondary Li-bearing mineral
671 (lithiophorite, cookeite) precipitation. A recent geostatistical study showed that most pegmatites occur
672 less than 500 m from a fault system (Deveaud et al, 2013).

673 **4.5 Grade assessment of and tonnage estimation**

674 **4.5.1 Data quality**

675 When regarding the available dataset, several problems are obvious. The differences in knowledge and
676 definition of mineral resources and reserves vary between historical data (St Austell, Beauvoir), JORC
677 (Jadar project) and NI43-101 (Alberta I project). Historical data estimates predate the CRIRSCO
678 system (before 1995; www.criirSCO.com). They are based on drilling campaigns managed by geological
679 surveys and related subsidiaries. Such data may lead to under- or over-estimates. Figure 11 shows that
680 projects and occurrences are distributed homogeneously despite their reference system (historical data
681 in italics *versus* CRIRSCO system in bold). Note that mineral resources from the St Austell deposits
682 appear to be strongly anomalous from the main population (Fig. 11, Table 4); they are unrealistic for
683 environmental and societal reasons, and probably not economically viable regarding ore grades. For
684 these reasons, the St Austell data are not used in the following sections. The JORC system, however,
685 may exclude some commercially sensitive information, such as mineral reserves if mineral resources
686 (Table 4), which is not allowed with the NI43-101 report. However, these points do not affect the
687 mineral resources comparison on which our estimates are based.

688 As mentioned above, thirteen projects in England (Meldon), Ireland (Aclare), France (Beauvoir,
689 Montebbras), Germany (Altenberg) and Ukraine were evaluated before setting up a “reporting system”,
690 as such mineral resource and -reserve estimates refer to historical evaluations. These data represent
691 only 5% of the entire dataset (Table 4). Fifteen projects were defined in the Australian JORC system
692 (e.g., Wolfsberg, Austria); one project (Zinnwald, Germany) in the European PERC; one in the
693 Canadian NI43-101 system (e.g., Alberta I project which comprises Presqueria deposit, Spain) and one
694 project is defined in the United Nation Framework Classification (UNFC; Alijo deposit).

695 However, we think that, despite the apparent discrepancies between reference systems, our dataset
696 is a good starting point for estimating the European Li hard-rock potential (Figs. 11, 12).

697 Moreover, Li-bearing minerals in lithiophorite and Li-chlorite occurrences in sedimentary
698 deposits—bauxite, Mn-(Fe), MVT and Li-bearing clay deposits—were not systematically described,
699 as Li was not of first interest at the time. This was the case in Spain, France and Turkey, and may hide
700 significant local Li grades, as in China (Wang et al., 2013) and USA (Tourtelot and Brenner-Tourtelot,
701 1977). Available data from bauxite deposits in China show that the average Li grade is very low

702 (2045 ppm Li_2O ; Wang et al, 2013). The same is true for Li-bearing shales in the Dauphinois area,
703 France, where the average Li content is 949.34 ppm Li_2O (Henry et al., 1996). Accordingly, these
704 occurrences can hardly be considered as potential Li deposits regarding their ore grade.

705 Based on the available dataset, 8,839,750 t of Li_2O (Table 4) are presently reported in Europe
706 from various deposit types and related to various Li-bearing minerals.

707 Furthermore, our study does not cover lithium in seawater, whose average content has been
708 estimated at 0.17 ppm (Fasel and Tran, 2005; Yaksic and Tilton, 2009), nor that potentially contained
709 in oilfields (e.g., Pechelbronn in France) and geothermal brines (e.g., the South Crofty deposit in the
710 UK; Cornish Lithium/Strongbow). Such potential lithium sources are difficult to quantify due to fluid
711 mixing, dilution and/or movement (Houston et al., 2011), but research is ongoing (e.g., Eramet-
712 IFPEN), as are potential resource estimates from such sources.

713 4.5.2 Range of ore grade and tonnage

714 At the deposit scale, metric tons of ore and average grades (Fig. 11, Table 4) of European hard-rock
715 lithium deposits are relatively competitive compared to the world-class LCT pegmatites from the
716 Greenbushes in Australia and Whabouchi in Canada, which are representative examples of such Li-
717 deposits. In detail, the Proterozoic Ukrainian pegmatites show similar grades and tonnages, whereas
718 Variscan pegmatites host lower tonnages. Thus, as pointed out before, significant differences in Li
719 content are seen among the various orogens. Interestingly, the Svecofennian, Sveconorwegian and
720 Variscan orogenies, which involved supercontinent accretion, continent-continent collision and
721 notable late lithospheric thickening, resulted in richer lithium deposits than the Cadomian, Caledonian
722 and Alpine orogenies. This suggests that processes involving extensive crustal anatexis from
723 lithospheric thickening lead to significant Li enrichment (Černý, 1991a, b). For the Alpine orogen, the
724 dearth in Li deposits could be related to a present-day deep erosional level, as indicated by the
725 presence of few LCT pegmatites emplaced at the highest structural levels, highlighted by miarolitic
726 (Guastoni et al., 2014, 2016) features (MI class of Černý and Ercit, 2005).

727 It also appears that greisen and RMG containing mainly Li-micas (lepidolite, zinnwaldite, Li-
728 muscovite) and Li-phosphates, may contain relatively higher tonnages, but lower grades, than the LCT
729 pegmatites, which contain mainly spodumene- and petalite-dominated Li-bearing minerals (Figs. 11,
730 12). This is, first, a function of deposit size: pegmatites are narrow and well constrained whereas
731 greisen and RMG can form kilometer-scale cupolas and may have deep roots (e.g., Beauvoir). Second,
732 the type of Li-bearing mineral, within which the Li_2O content may vary significantly (Table 1), is
733 another major parameter, illustrated by spodumene *versus* zinnwaldite.

734 Finally, in addition to the above points, ore grade can be controlled by several other parameters.
735 These include the geochemistry of fluxing fluids (F, B and P), different crystallization parameters and

736 P-T conditions (spodumene *versus* petalite; Černý and Ferguson, 1972), and variable degrees of
737 fractionation (Li-phosphate occurrences against amblygonite-montebrazite or triphylite-sicklerite-
738 ferrisicklerite series; Černý, 1991b). All these may affect the number and type of Li-bearing minerals,
739 as well as their mineral size and relative abundance, and therefore the overall Li content.

740 4.6 Perspectives

741 As emphasized by this study, lithium in hard-rock deposits is not rare in Europe and well distributed
742 within Proterozoic to Cenozoic orogens (Fig. 8). The Variscan orogeny (Fig. 6) shows the most
743 important Li-content (more than 60% of the identified deposits in Table 4) in various deposit types
744 (greisen, RMG, pegmatite). The oldest orogens mainly contain LCT pegmatites (Figs. 3, 5) that tend to
745 cluster, potentially because of successive orogenic reworking. However, only very few studies report
746 lithium occurrences related to young Mediterranean orogens, suggesting either a lack of exploration or
747 a significant difference between the Variscan and Alpine orogenies.

748 As for jadarite occurrences, greenfield exploration in Balkan countries such as Serbia and Bosnia
749 may identify latent deposits related to lacustrine evaporite basins. Currently, this area is relatively
750 underexplored and several exploration and mining companies showed recent interest in acquiring
751 permits, such as the Australian firm South East Asia Resources, recently renamed Jadar Lithium.

752 Regarding Li-production, LCT pegmatites that generally have high lithium grades and low
753 tonnages could be rapidly in production as Li-extraction processes for spodumene are operational.
754 Greisen and RMG, which have low Li grades and high tonnages, will take somewhat longer to reach
755 production as the extraction processes of Li-bearing micas must be demonstrated at deposit scale.

756

757 5. Conclusions

758 This review of Li hard-rock lithium metallogeny in Europe demonstrates that a wide range of deposit
759 types, including endogenous (LCT pegmatites, RMG, greisen) and exogenous (Jadar, bauxite)
760 processes, is involved. The lithium is contained in various Li-bearing minerals, such as spodumene,
761 lepidolite and zinnwaldite, which are related to different orogenies through time. A favorable
762 geodynamic setting for endogenous magmatic lithium accumulation comprises a late orogenic process,
763 commonly postdating arc accretion, coeval with continent-continent collision, and related to local
764 crustal thickening. A post-orogenic extensional setting is favorable for exogenous processes that can
765 concentrate lithium into a deposit.

766 At present, 27 potential hard-rock deposits have been identified in Europe. The sum of such Li
767 resources is estimated at 8,839,750 t of Li₂O. Their production may secure, in part, European lithium
768 requirements in the near future.

769 Our inventory also reflects the heterogeneity in knowledge regarding lithium occurrences. This is
770 due to a relative lack of interest in lithium until recently and suggests that new targets might be
771 defined in the foreseeable future through active ongoing exploration.

772

773 6. Acknowledgements

774 We gratefully acknowledge Drs. Mali H., Uher P., and Ilickovic T. for their assistance regarding
775 European occurrence locations. We also thank Matevž Novak from the Geological Survey of Slovenia
776 for the use of the jadarite picture. This study was funded by the French Centre for Excellence
777 Voltaire* - LABEX VOLTAIRE (Geofluids and VOLatils, Earth, Atmosphere - Resources and
778 Environment) in collaboration with the French geological survey (BRGM) and the Economic
779 Laboratory of Orléans University (LEO). We thank two anonymous reviewers and Dr. Seltmann for
780 their constructive comments that greatly helped to improve the manuscript. Dr. H.M. Kluijver edited
781 the final English version of the MS.

782

783 7. References

784 Ackerman L., Haluzová E., Creaser R.A., Pašava J., Veselovský F., Breiter K., Erban V., and Drábek
785 M., 2017. Temporal evolution of mineralization events in the Bohemian Massif inferred from the Re-
786 Os geochronology of molybdenite; *Mineralium Deposita*, Vol. 52, 651-662. <https://doi.org/10.1007/s00126-016-0685-5>.

788 Alviola R., Mänttari I., Mäkitie H., and Vaasjoki, M., 2001. Svecofennian rare-element granitic
789 pegmatites of the Ostrobothnia region, western Finland: their metamorphic environment and time of
790 intrusion; *In Svecofennian granitic pegmatites (1.86-1.79 Ga) and quartz monzonite (1.87 Ga), and
791 their metamorphic environment in the Seinäjoki region, western Finland, Mäkitie H. (eds.); Geological
792 Survey of Finland. Special Paper 30, 9-29.*

793 Anderson S.T., 2015. The mineral Industry of Hungary; *In 2012 Yearbook, Hungary, USGS Science
794 for a changing world, 8p.*

795 Armand M., and Tarascon J.M., 2008. Building better batteries; *Nature*, Vol.451, 652-657.

796 Artemieva I.M., Thybo H. and, Kaban M.K., 2006. Deep Europe today: geophysical synthesis of the
797 upper mantle structure and lithospheric processes over 3.5 Ga; *Memoirs of the Geological Society of
798 London*, Vol. 32, 11-41.

799 Artemieva I.M., and Thybo H., 2013. EUNaseis: A seismic model for Moho and crustal structure in
800 Europe, Greenland, and the North Atlantic region, *Tectonophysics*, Vol. 609, 97-153.

- 801 Aubert G., 1969. Les coupoles granitiques de Montebas et d'Echassières (Massif Central français) et
802 la genèse de leurs minéralisations en étain, lithium, tungstène et béryllium; Mémoire BRGM, 46,
803 345pp.
- 804 Bardossy G., 1982. Karst bauxites, Bauxite deposits on carbonate rocks; *In* Developments in economic
805 geology, Elsevier Scientific publishing company (eds.), Vol.14, 442p.
- 806 Barros R., 2017. Petrogenesis of the Leinster LCT (Li-Cs-Ta) pegmatite belt in southeast Ireland; PhD
807 Thesis, University College Dublin, Ireland, 287 p.
- 808 Barros R. and Menuge J.F., 2016. The origin of spodumene pegmatites associated with the Leinster
809 granite in southeast Ireland; *The Canadian Mineralogist*, Vol. 54, 847-862
- 810 Beltrando M., Frasca G., Compagnoni R., and Vitale-Brovarone A., 2012. The Valaisian controversy
811 revisited: multi-stage folding of a Mesozoic hyper-extended margin in the Petit St. Bernard pass area
812 (Western Alps); *Tectonophysics*, Vol. 579, 17-36.
- 813 Bergh S.G., Corfu F., Priyatkina N., Kullerud K. and Myhre P.I., 2015. Multiple post-Svecofennian
814 1750-1560 Ma pegmatite dykes in Archean-Paleoproterozoic rocks of the West Troms Basement
815 Complex, North Norway: Geological significance and regional implications; *Precambrian Research*,
816 Vol. 266, 425-439.
- 817 Bertotti G., Seward D., Wijbrans J., Ter Voorde M., and Hurford A.J., 1999. Crustal thermal regime
818 prior to, during, and after rifting: a geochronological and modelling study of the Mesozoic South
819 Alpine rifted margin; *Tectonics*, Vol. 18, 185-200.
- 820 Bongiolo E.M., Renac C., d'Almeida de Toledo Piza P., da Silva Schmitt R., and Sampaio Mexias A.,
821 2016. Origin of pegmatites and fluids at Ponta Negra (RJ, Brazil) during late- to post-collisional stages
822 of the Gondwana Assembly. *Lithos*, 240–243, 259–275.
- 823 Bonin, B., 1998. Orogenic to non-orogenic magmatic events: Overview of the Late Variscan
824 magmatic evolution of the Alpine Belt; *Turkish Journal of Earth Sciences*, Vol. 7; 133-143.
- 825 Bousquet R., Schmid S.M., Zeilinger G., R., Rosenberg C., Molli G., Robert C., Wiederkehr M., and
826 Rossi P., 2012. Tectonic framework of the Alps, Scale 1:1,000,000; Commission for the Geological
827 Map of the World.
- 828 Bradley D.C., Munk L., Jochens H., Hynek S., and Labay K., 2013. A preliminary deposit model for
829 lithium brines; U.S. Geological Survey, Open File Report 2013-1006, 9.
- 830 Bradley D.C., 2011. Secular trends in the geologic record and the supercontinent cycle; *Earth-Science*
831 *Reviews*, Vol. 108, 16-33.

- 832 Braux C., Piantone P., Zeegers H., Bonnemaïson M., and Prévot J.C., 1993. Le Châtelet gold-bearing
833 arsenopyrite deposit, Massif Central France: Mineralogy and geochemistry applied to prospecting;
834 Applied Geochemistry, Vol. 8, 339-356.
- 835 Breiter, K., Korbeloca Z., Chladek S., Uher P., Knesl I., Rambousek P., Honig S., and Sesulka V.,
836 2017. Diversity of Ti-Sn-W-Nb-Ta oxide minerals in the classic granite-related magmatic-
837 hydrothermal Cinovec/Zinnwald Sn-W-Li deposit (Czech Republic); European Journal of Mineralogy,
838 Vol. 29, 727-738.
- 839 BRGM, 2017. Le lithium (Li) – éléments de criticité, fiche de synthèse sur la criticité des matières
840 minérales – le lithium ; Mineral Info, 8 p.
- 841 British Geological Survey, 2016. Lithium; Minerals UK, Mineral profile, 39 p.
- 842 Bussink R.W., 1984. Geochemistry of the Panasqueira tungsten-tin deposit, Portugal; PhD thesis,
843 University of Utrecht, The Netherlands, 170 p.
- 844 Cameron E.N., Jahns R.H., McNair A.H. and Page L.R., 1949. Internal structure of granitic
845 pegmatites. Economic Geology Monograph 2, 115 p.
- 846 Cassard D., Bertrand G., Billa M., Serrano J.J., Tourlière B., Angel J.M., and Gaal G., 2015. ProMine
847 Mineral Databases: New tools to assess primary and secondary mineral resources *In* 3D, 4D and
848 Predictive Modelling of Major Mineral Belts in Europe, Weihed P., (ed.); Mineral Resource Reviews,
849 DOI 10.1007/978-3-319-17428-0_2
- 850 Černý P., 1992. Regional zoning of pegmatite populations and its interpretation; Mitteilungen der
851 Österreichischen Mineralogischen Gesellschaft, Vol. 137, 99-107.
- 852 Černý P., 1991a. Rare-element granitic pegmatites. Part 1: Anatomy and internal evolution of
853 pegmatite deposits; Geoscience Canada, Vol. 18, 49-67.
- 854 Černý P., 1991b. Rare-element granitic pegmatites. Part 2: Regional to global environments and
855 petrogenesis; Geoscience Canada, Vol. 18, 68-81.
- 856 Černý P., 1990. Distribution, affiliation and derivation of rare-element granitic pegmatites in the
857 Canadian Shield; Geologische Rundschau, Vol. 79, 183-226.
- 858 Černý P., 1989. Characteristics of pegmatite deposits of tantalum; *In* Lanthanides, Tantalum and
859 Niobium, Möller P., Černý P., and Saupé F., (eds.); Society for Geology applied to Mineral deposits,
860 Special Publication 7, Springer-Verlag, 192-236.

- 861 Černý P. and Ercit T.S., 2005. The classification of granitic pegmatites revisited; *The Canadian*
862 *Mineralogist*, Vol. 43, 2005-2026.
- 863 Černý P., and Ferguson R.B., 1972. The Tanco pegmatite at Bernic Lake, Manitoba. IV. Petalite and
864 Spodumene relations; *The Canadian Mineralogist*, Vol. 11, 660-678.
- 865 Černý P., London D. and Novák M., 2012. Granitic pegmatites as reflections of their sources;
866 *Elements*, Vol. 8, 289-294.
- 867 Cháb J., 2010. Outline of the geology of the Bohemian Massif: The basement rocks and their
868 Carboniferous and Permian cover; Czech Geological Survey, Prague, 295 p.
- 869 Charles N., Tuduri J., Guyonnet D., Melleton J., and Pourret O., 2013. Rare earth elements in Europe
870 and Greenland: a geological potential? An overview; *Mineral Deposit Research for a high-Tech*
871 *World*, 12th SGA Biennial meeting, Vol. 4, 4 p.
- 872 Charoy B., and Noronha F., 1996. Multistage growth of rare-element, volatile-rich microgranite at
873 Argemela (Portugal); *Journal of Petrology*, Vol. 37, 73-94.
- 874 Charoy B., and Noronha F., 1991. The Argemela granite-porphyry (Central Portugal): the subvolcanic
875 expression of a high-fluorine, rare-element pegmatite magma; *In Source, Transport and deposition for*
876 *metals*, Pagel M., and Leroy J.L., (Eds.), 741-744.
- 877 Christman P., Gloaguen E., Labbé J.F., Melleton J., and Piantone P., 2015. Global lithium resources
878 and sustainability issues; *In Lithium Process Chemistry, Resources, Extraction, Batteries and*
879 *Recycling*, Chagnes A. and, Switowska J., (eds.); Elsevier, 1-40.
- 880 Clark L., 1963. The geology and petrology of the Ennerdale granophyre. Its metamorphic aureole and
881 associated mineralization; PhD thesis, University of Leeds, England, 324 p.
- 882 Cotterell T., 2009. Supergene manganese mineralization associated with the Camdwr fault in the
883 Central Wales orefield; *Journal of the Russell Society*, Vol.12, 15-25.
- 884 Cuney M. and Autran A., 1987. Objectifs généraux du projet GPF Echassières n°1 et résultats
885 essentiels acquis par le forage de 900 m sur le granite albitique à topaze-lépidolite de Beauvoir; *In:*
886 *Cuney M. and Autran A. (Eds), Echassières. Le forage scientifique d'Echassières: une clé pour la*
887 *compréhension des mécanismes magmatiques et hydrothermaux associés aux granites à métaux rares;*
888 *Mémoire Géologie de la France (GPF) 1, 7-24.*
- 889 Cuney M., and Barbey P., 2014. Uranium , rare metals, and granulite-facies metamorphism;
890 *Geoscience Frontiers*, Vol. 5, 1-17.

- 891 Cuney M., Marignac C. and Weisbrod A., 1992. The Beauvoir topaz-lepidolite albite granite (Massif
892 Central, France): The disseminated magmatic Sn-Li-Ta-Nb-Be mineralization; *Economic Geology*,
893 Vol. 87, 1766-1794.
- 894 Cuney M., Alexandrov P., Le Carlier de Veslud C., Cheilletz A., Raimbault L., Ruffet G. and Scaillet
895 S., 2002. The timing of W-Sn –rare metals mineral deposit formation in the Western Variscan chain in
896 their orogenic setting: the case of the Limousin area (Massif Central, France); *In The Timing of Major*
897 *Ore Deposits in an Evolving Orogeny*, Blundell D.J., Neubauer E. and Von Quadt A. (eds); Geological
898 Society, London, Special Publications, Vol. 204, 213-228.
- 899 Dakota Minerals Ltd., 2017. Sepeda – Largest Pegmatite-Hosted JORC Lithium Resource in Europe;
900 ASX announcement, 20 February 2017; press release, 29 p.
- 901 D’Argenio B., and Mindszenty A., 1986. Cretaceous bauxites in the tectonic framework of the
902 Mediterranean; *Rendiconti della Società Geologica Italiana di Mineralogia e Petrologia*, Vol. 9, 257-
903 262.
- 904 Deveaud S., Millot R., and Villaros A., 2015. The genesis of LCT-type granitic pegmatites, as
905 illustrated by lithium isotopes in micas; *Chemical Geology*, Vol. 411, 97-101.
- 906 Deveaud S., 2015. Caractérisation de la mise en place des champs de pegmatites à éléments rares de
907 type LCT – Exemples représentatifs de la chaîne Varisque; PhD thesis, University of Orléans, France,
908 350 p.
- 909 Deveaud S., Gumiaux C., Gloaguen E., and Branquet Y., 2013. Spatial statistical analysis applied to
910 rare-elements LCT pegmatite fields: An original approach to constrain fault-pegmatites-granites
911 relationships; PEG 2013, 6th International Symposium on Granitic Pegmatites, Program with abstract,
912 36.
- 913 Deveaud S., Gumiaux C., Gloaguen E., and Branquet Y., 2013. Spatial statistical analysis applied to
914 rare-element LCT type pegmatite fields: An original approach to constrain faults-pegmatites-granites
915 relationships; *Journal of Geosciences*, Vol. 58, 163-182.
- 916 Eilu P., Ahtola T., Äikäs O., Halkoaho T., Heikura P., Hulkki H., Iljina M., Juopperi H., Karinen T.,
917 Kärkkäinen N., Konnunaho J., Kontinen A., Kontoniemi O., Korkiakoski E., Korsakova M.,
918 Kuivasaari T., Kyläkoski M., Makkonen H., Niiranen T., Nikander J., Nykänen V., Perdahl J.A.,
919 Pohjolainen E., Räsänen J., Sorjonen-Ward P., Tiainen M., Tontti M., Torppa A., and Västi K., 2012.
920 Metallogenic areas in Finland; Geological Survey of Finland, Special Paper 53, 207-342.
- 921 Ericksen G.E., and Salas R., 1987. Geology and resources of salars in the central Andes; U.S.
922 Geological Survey, Open File Report. 88–210, 51.

- 923 Ertl A., Schuster R., Hughes J.M., Ludwig T., Meyer H.P., Finger F., Dyar M.D., Ruschel K.,
924 Rossman G.R., Klötzli U., Brandstätter F., Lengauer C.L., and Tillmanns E., 2012. Li-bearing
925 tourmalines in Variscan granitic pegmatites from the Moldanubian nappes, Lower Austria; *European*
926 *Journal of Mineralogy*, Vol. 24, 695-715.
- 927 Fasel D., and Tran M.Q., 2005. Availability of lithium in the context of future D-T fusion reactors;
928 *Fusion Engineering and Design*, Vol. 75-79, 1163–1168.
- 929 Faure M., Bé Mézène E., Duguet M., Cartier C., and Talbot J.Y., 2005. Paleozoic tectonic evolution of
930 Medio-Europa from the example of the French Massif Central and Massif Armoricaïn; *Journal of the*
931 *Virtual Explorer*, Vol. 19, 26 p.
- 932 Ferrara G., and Tonarini S., 1985. Radiometric geochronology in Tuscany: Results and problems;
933 *Rendiconti della Società Italiana di Mineralogia e Petrologia*, Vol. 40, 111-124.
- 934 Fritschle T., 2016. Age and origin of late Caledonian granites and Ordovician arc magmatic rocks in
935 Ireland and the Isle of Man; PhD thesis, University College, Dublin, Ireland, 359 p.
- 936 Finger F., Gerdes A., Janousek V., René M., and Riegler G., 2007. Resolving the Variscan evolution
937 of the Moldanubian sector of the Bohemian Massif: The significance of the Bavarian and the Moravo-
938 Moldanubian tectonometamorphic phases; *Journal of Geosciences*, Vol. 52, 9-28.
- 939 Finger F., Broska I., Haunschmid B., Hrasko L., Kohút M., Krenn E., Petrik I., Riegler G., Cassiterite
940 U-Pb geochronology constrains magmatic-hydrothermal evolution in complex evolved granite
941 systems: The classic Erzgebirge Tin Province (Saxony and Bohemia) Electron-microprobe dating of
942 monazites from Western Carpathian basement granitoids: plutonic evidence for an important Permian
943 rifting event subsequent to Variscan crustal anatexis; *International Journal of Earth Sciences*, Vol. 92,
944 86-98.
- 945 Gallego Garrido M., 1992. Las mineralizaciones de Li asociadas a magmatismo ácido en Extremadura
946 y su encuadre en la Zona Centro-Ibérica; PhD thesis, Universidad Complutense, Madrid, Spain, 342 p.
- 947 Garfunkel Z., 2015. The relations between Gondwana and the adjacent peripheral Cadomian domain-
948 constrains on the origin, history and paleogeography of the peripheral domain; *Gondwana Research*,
949 Vol. 28, 1257-1281.
- 950 Gébelin A., Roger F., and Brunel M., 2009. Syntectonic crustal melting and high-grade metamorphism
951 in a transpressional regime, Variscan Massif Central, France; *Tectonophysics*, Vol. 477, no 3–4,
952 229-43. <https://doi.org/10.1016/j.tecto.2009.03.022>.
- 953 Gébelin A., Brunel M., Monié P., Faure M., and Arnaud N., 2007. Transpressional tectonics and
954 Carboniferous magmatism in the Limousin, Massif Central, France: Structural and $^{40}\text{Ar}/^{39}\text{Ar}$
955 Investigations; *Tectonics*, Vol. 26, 2, 27 p. <https://doi.org/10.1029/2005TC001822>.

- 956 Gee D.G., Bogolepova O.K., and Lorenz H., 2006. The Timanide, Caledonide and Uralide orogens in
957 the Eurasian high Arctic, and relationships to the palaeo-continent Laurentia, Baltica and Siberia; *In*
958 *European Lithosphere of Dynamics*, Gee D.G. and Stephenson, R.A. (Eds): Geological Society,
959 London, Memoirs, 32, 507–521.
- 960 Glanzman R.K., McCarthy Jr. J.H., and Rytuba J.J., 1978. Lithium in the McDermitt Caldera, Nevada
961 and Oregon; *Energy*, Vol. 3, 347-353.
- 962 Guastoni A., Pozzi G., Secco L., Schizza M., Pennacchioni G., Fioretti A.M. and, Nestola F., 2016.
963 Monazite-(Ce) and xenotime-(Y) from an LCT, NYF tertiary pegmatite field: evidence from a regional
964 study in the Central Alps (Italy and Switzerland); *The Canadian Mineralogist*, Vol. 54, 863-877.
- 965 Guastoni A., Pennacchioni G., Pozzi G., Fioretti A.M., and Walter J.M., 2014. Tertiary pegmatite
966 dikes of the Central Alps; *The Canadian Mineralogist*, Vol. 52, 191-219.
- 967 Heinrich C.A., 1990. The chemistry of hydrothermal tin (-tungsten) ore deposition; *Economic*
968 *Geology*, Vol. 85, 457-481.
- 969 Henry C., Burkhard M., and Goffré B., 1996. Evolution of synmetamorphic veins and their wallrocks
970 through a Western Alps transect: No evidence for large-scale flow. Stable isotope, major- and trace-
971 element systematics; *Chemical Geology*, Vol. 127, 81-109.
- 972 Hofstra A.H., Todorov T., Mercer C., Adams D., and Marsh E., 2013. Silicate melt inclusion evidence
973 for extreme pre-eruptive enrichment and post-eruptive depletion of lithium in silicic volcanic rocks of
974 the Western United States: Implications for the origin of lithium-rich brines; *Economic Geology*,
975 Vol. 108, 1691-1701.
- 976 Hollinger P., Cuney M., Friedrich M., and Turpin L., 1986. Age carbonifère de l'unité de Brame du
977 complexe granitique peralumineux de Saint-Sylvestre (NO du Massif Central) défini par les données
978 isotopiques U-Pb sur zircon et monazite; *Académie des Sciences, Comptes rendus, series II*, Vol. 303,
979 1309-1314.
- 980 Houston J., Butcher A., Ehren P., Evans K., and Godfrey L., 2011. The evaluation of brine prospects
981 and the requirement for modifications to filing standards; *Economic Geology*, Vol. 106, 1225-1239.
- 982 Ilickovic T., Schuster R., Mali H., Petrakakis K., Schedl A., and Horschinegg M., 2016. Spodumene
983 bearing pegmatites in the Austroalpine unit (Eastern Alps): New field observations and
984 geochronological data; *GeoTirol, Abstract with Poster*, 138.
- 985 Ilickovic T., Schuster R., Mali H., Petrakakis K., and Schedl A., 2017. Spodumene bearing pegmatites
986 in the Austroalpine unit (Eastern Alps): Distribution and new geochronological data; *Geophysical*
987 *Research Abstracts*, EGU2017-7235, Vol. 19, Program with Abstract.

- 988 Jackson B., 1982. An occurrence of gem quality elbaite from Glenbuchat, Aberdeenshire, Scotland;
989 Journal of Gemmology, Vol. 2, 121-125.
- 990 Jahns R.H., and Burnham C.W. 1969. Experimental studies of pegmatites gneiss: A model for the
991 derivation and crystallization of granitic pegmatities; Economic Geology, Vol. 64, 843-864.
- 992 Jarchovský T., 2006. The nature and genesis of greisen stocks at Krasno, Slavkovsky les area –
993 western Bohemia, Czech Republic; Journal of the Czech Geological Society, Vol. 51, 16 p.
- 994 Johan Z., and Johan V., 2005. Accessory minerals of the Cinovec (Zinnwald) granite cupola, Czech
995 Republic: Indicators of petrogenetic evolution; Mineralogy and Petrology, Vol. 83, 113-150.
- 996 Jolivet L., Faccenna C., and Piromallo C., 2009. From mantle to crust: Stretching the Mediterranean;
997 Earth and Planetary Science Letters, Vol. 285, 198-209.
- 998 Johnson T.E., Hudson N.F.C., and Droop G.T.R., 2001. Melt segregation structures within the Inzie
999 Head gneisses of the northeastern Daldarian; Scottish Journal of Geology, Vol. 37, 59-72.
- 1000 Jullien M., and Goffé B., 1993. Occurrences de cookéite et de pyrophyllite dans les schistes du
1001 Dauphinois (Isère, France) - Conséquences sur la répartition du métamorphisme dans les zones extemes
1002 alpines. Schweiz; Mineralogy and Petrology, Vol. 73, 357-363.
- 1003 Kesler S.E., Gruber P.W., Medina P.A., Keoleian G.A., Everson M.P., and Wallington T.J., 2012.
1004 Global lithium resources: relative importance of pegmatite, brine and other deposits; Ore Geology
1005 Reviews, Vol. 48, 55-69.
- 1006 Kohút M., and Stein H., 2004. Re-Os molybdenite dating of granite-related Sn-W-Mo mineralisation
1007 at Hnilec, Germeric Superunit, Slovakia; Mineralogy and Petrology, Vol. 85, 117-129.
- 1008 Koistinen T., Stephens M.B., Bogatchev V., Nordgulen Ø., Wennerström M., and Korhonen J., 2001.
1009 Geological Map of the Fennoscandian Shield, Scale 1:2,000,000; Espoo, Geological Survey Finland;
1010 Geological Survey Norway, Geological Survey Sweden, Ministry of Natural Resources of Russia,
1011 Moscow.
- 1012 Kontak D.J., Dostal J., Kyser T.K. and Archibald D.A., 2002. A petrological, geochemical, isotopic
1013 and fluid inclusion study of 370 Ma pegmatite-aplite sheets, Peggys Cove, Nova Scotia, Canada; The
1014 Canadian Mineralogist, Vol. 40, 1249–1286.
- 1015 Korja, A., Lahtinen, R. and Nironen, M. 2006. The Svecofennian orogen—a collage of
1016 microcontinents and island arcs; *In* European Lithosphere Dynamics, Gee D.G., and Stephenson R.A.
1017 (Eds.); Geological Society, London, Memoirs, Vol. 32, 561–578.

- 1018 Kovács I., Csontos L., Szabó C., Bali E., Falus G., Benedek K., and Zajacz Z., 2007. Paleogene-Early
1019 Miocene igneous rocks and geodynamics of the Alpine-Carpathian-Pannonian-Dinaric region: An
1020 integrated approach; Geological Society of America Special Paper 41, 93 p.
- 1021 Kroner U., and Romer R.L., 2013. Two plates – Many subductions zones: The Variscan orogeny
1022 reconsidered; Gondwana Research, Vol. 24, 298-329.
- 1023 Kulp J.L., Kologrivov R, Engels J., Catanzaro E.J., Neumann H., and Nilssen B., 1963. Age of the
1024 Tordal, Norway pegmatite - a correction; Geochimica et Cosmochimica Acta, Vol. 27, 847-848.
- 1025 Kuusela J., Ahtola T., Koistinen E., Seppänen H., Hatakka T., and Lohva J., 2011. Report of
1026 investigations on the Rapasaaret lithium pegmatite deposit in Kaustine-Kokkola, Western Finland;
1027 GTK Southern Finland Office, 42/2011, 65 p.
- 1028 Kurhila M., Vaasjoki M., Mänttari I., Rämö T., and Nironen M., 2005. U-Pb ages and Nd isotope
1029 characteristics of the late orogenic, migmatizing microcline granites in southwestern Finland; Bulletin
1030 of the Geological Society of Finland, Vol. 77, 105-128.
- 1031 Kvasnista V.N., Silaev V.I., and Smoleva I.V., 2016. Carbon isotopic composition of diamonds in
1032 Ukraine and their probable polygenetic nature; Geochemistry International, Vol. 54, 948-963.
- 1033 Lahtinen R., Korja A., Nironen M., and Heikkinen P., 2009. Palaeoproterozoic accretionary processes
1034 in Fennoscandia; Geological Society of London, Special Publications, Vol. 318, 237-256.
1035 DOI: 10.1144/SP318.8
- 1036 Launay G., Sizaret S., Guillou-Frottier L., Fauguerolles C., Champallier R., and Gloaguen E., 2019.
1037 Dynamic permeability related to greisenization reactions in Sn-W ore deposits: Quantitative
1038 petrophysical and experimental evidence; Geofluids, Vol. 2019, 23p.
- 1039 Lecomte A., Cathelineau M., Deloule E., Brouand M., Peiffert C., Loukola-Ruskeeniemi K.,
1040 Pohjolainen E., and Lahtinen H., 2014. Uraniferous bitumen nodules in the Talvivaara Ni-Zn-Cu-Co
1041 deposit (Finland): Influence of metamorphism on uranium mineralization in black shales; Mineralium
1042 Deposita, Vol. 49, 513-533.
- 1043 Lehmann B., 1994. Granite-related rare-metal mineralization: a general geochemical framework; *In*
1044 *Metallogeny of Collisional Orogens*, Seltmann, Kämpf and Möller (eds.); Czech Geological Survey,
1045 Prague, 342-349.
- 1046 Lindroos A., Romer R.L., Ehlers C., and Alviola R., 1996. Late-orogenic Svecofennian deformation in
1047 SW Finland constrained by pegmatite emplacement ages; Terra Nova, Vol. 8, 567-574.
- 1048 Linnemann U., Pereira F., Jeffries T.E., Drost K., and Gerdes A., 2008. The Cadomian orogeny and
1049 the opening of the Rheic Ocean: The diachrony of geotectonic processes constrained by LA-ICP-MS U-

- 1050 Pb zircon dating (Ossa-Morena and Saxo-Thuringian Zones, Iberian and Bohemian Massifs);
1051 Tectonophysics, Vol. 461, 21-43.
- 1052 Linnemann U., Pereira F., Jeffries T.E., Drost K., and Gerdes A., 2007. The continuum between
1053 Cadomian orogenesis and opening of the Rheic Ocean: constraints from LA-ICP-MS U-Pb zircon
1054 dating and analysis of plate-tectonic setting (Saxo-Thuringian Zone, NE Bohemian Massif, Germany);
1055 *In* The Evolution of the Rheic Ocean: from Avalonian–Cadomian Active Margin to Alleghenian–
1056 Variscan Collision, Linnemann U., Nance D., Kraft P., and Zulauf G. (Eds.); Geological Society of
1057 America, Boulder, Colorado, 61-96.
- 1058 Linnen R.L., van Litchtervelde M., and Černý P., 2012. Granitic pegmatites as sources of strategic
1059 metals; Elements, Vol. 8, 275-280.
- 1060 Linnen R.L., and Cuney M., 2005. Granite-related rare-element deposits and experimental constraints
1061 on Ta-Nb-W-Sn-Zr-Hf mineralization; *In* Rare-Element Geochemistry and Mineral Deposits, Linnen,
1062 R.L. and Samson, I.M. (Eds.), Vol. 17, Geological Association of Canada Short Course Notes, 45-68.
- 1063 Lima A., 2000. Estrutura, Mineralogia e Génese dos Filões Aplitopegmatíticos com Espodumena da
1064 Região do Barroso-Alvão (Norte de Portugal); PhD thesis, University of Porto, Portugal, and INPL,
1065 Nancy, France, 270 p.
- 1066 London D., 2018. Ore-forming processes within granitic pegmatites; Ore Geology Reviews, Vol. 101,
1067 349-383.
- 1068 London D., 2008. Pegmatites; The Canadian Mineralogist Special Publication Vol. 10, 347 pp.
- 1069 London D., 2005. Granitic pegmatites – An assessment of current concepts and directions for the
1070 future; Lithos, Vol.80, 281-303.
- 1071 London D., 1995. Geochemical features of peraluminous granites, pegmatites, and rhyolites as source
1072 of lithophile metal deposits; Mineralogical Association of Canada Short Course Handbook, Vol. 23,
1073 175-202.
- 1074 London D., 1992. The application of experimental petrology to the genesis and crystallization of
1075 granitic pegmatites; The Canadian Mineralogist, Vol. 77, 129-145.
- 1076 London D., 1990. Internal differentiation of rare element pegmatites; A synthesis of recent research;
1077 Geological Society of America, Special Paper 246, 35-50.
- 1078 London D., 1986. Magmatic –hydrothermal transition in the Tanco rare-element pegmatite: Evidence
1079 from fluid inclusions and phase-equilibrium experiments; American Mineralogist, Vol. 71, 376-395.
- 1080 Luecke W., 1981. Lithium pegmatites in the Leinster Granite (southeast Ireland); Chemical Geology,
1081 Vol. 34, 195-233.

- 1082 Lulzac Y., and Apolinarski F., 1986. Inventaire du territoire métropolitain les minéralisations à étain,
1083 tantale et lithium de Tréguennec (Finistère), état des connaissances au 31 mars 1986; BRGM Report
1084 86 DAM 011 OP4, 37 p.
- 1085 Manthiram A., Yu X., and Wang S., 2017. Lithium battery chemistries enabled by solid-state
1086 electrolytes; *Nature Reviews Materials*, Vol. 2, 16103.
- 1087 Matte P., 1991. Accretionary history and crustal evolution of the Variscan belt in Western Europe;
1088 *Tectonophysics*, Vol. 196, 309-337.
- 1089 Matte P., Maluski H., Rajlich P., and Franke W., 1990. Terrane boundaries in the Bohemian Massif;
1090 Result of a large scale Variscan shearing; *Tectonophysics*, Vol. 177, 151-170.
- 1091 Matte P., 1986. La chaîne varisque parmi les chaînes paléozoïques péri atlantiques, modèle d'évolution
1092 et position des grands blocs continentaux au Permo-Carbonifère; *Bulletin de la Société géologique de*
1093 *France*, II, 9-24.
- 1094 Marcoux E., 2017. Mines et ressources minérales en Armorique; Société de l'industrie minérale,
1095 472 p. ISBN 978-2-91-835001-9
- 1096 Marignac C., and Cuney M., 1999. Ore deposits of the French Massif Central: Insight into the
1097 metallogenesis of the Variscan collision belt; *Mineralium Deposita*, Vol. 34, 472-504.
- 1098 Martín-Izard A., Reguilón R., and Palero F., 1992. Cassiterite U-Pb geochronology constrains
1099 magmatic-hydrothermal evolution in complex evolved granite systems: The classic Erzgebirge Tin
1100 Province (Saxony and Bohemia) Martínez Catalán J.R., 1990. A non-cylindrical model for the
1101 northwest Iberian allochthonous terranes and their equivalents in the Hercynian belt of Western
1102 Europe; *Tectonophysics*, Vol. 179, 253–272.
- 1103 Martin R.F., and De Vito C., 2005. The patterns of enrichment in felsic pegmatites ultimately depend
1104 on tectonic setting: *The Canadian Mineralogist*, Vol. 43, 2027–2048.
- 1105 McKerrow W.S., MacNiocail C., and Dewey J.T., 2000. The Caledonian orogeny redefined; *Journal*
1106 *of the Geological Society, London*, Vol. 157, 1149–1154.
- 1107 Melleton J., Gloaguen E., and Frei D., 2015. Rare-elements (Li-Be-Ta-Sn-Nb) magmatism in the
1108 European Variscan belt, a review; *SGA 2015: Ressources minérales dans un monde durable*, Nancy,
1109 France.
- 1110 Melleton J., Gloaguen E., Frei D., Novák M., and Breiter K., 2012. How are the emplacement of rare-
1111 element pegmatites, regional metamorphism and magmatism interrelated in the Moldanubian Domain
1112 of the Variscan Bohemian Massif Czech Republic; *The Canadian Mineralogist*, Vol. 50, 1751-1773.

- 1113 Melleton J., Gloaguen E., Frei D., Lima A., 2011. U-Pb dating of columbite–tantallite from Variscan
1114 rare- elements granites and pegmatites; *Mineral. Mag.*, Vol. 75, 1452 p.
- 1115 Menant A., Jolivet L., Tuduri J., Loiselet C., Bertrand G., and Guillou-Frottier L., 2018. 3D
1116 subduction dynamics: A first-order parameter of the transition from copper- to gold-rich deposits in
1117 the eastern Mediterranean region; *Ore Geology Reviews*, Vol. 94, 118-135.
- 1118 Miles A.J., Woodcock N.H., and Hawkesworth C.J., 2016. Tectonic controls on post-subduction
1119 granite genesis and emplacement: The Late Caledonian suite of Britain and Ireland; *Gondwana*
1120 *Research*, Vol. 39, 250-260.
- 1121 Mohr S., Mudd G.M., and Giurco D.P., 2012. Lithium resources and production: Critical assessment
1122 and global projections; *Minerals*, Vol. 2, 65-84.
- 1123 Mudd G.M., and Jowitt S.M., 2016. From mineral resources to sustainable mining – the key trends to
1124 unlock the Holy Grail; In *Proceedings of the Third AusIMM International Geometallurgy Conference*
1125 *(GeoMet) 2016*, pp 37–54 (The Australasian Institute of Mining and Metallurgy: Melbourne).
- 1126 Müller A., Ihlen P.M., Snook B., Larsen R.B., Flem B., Bingen B., and Williamson B.J. 2015. The
1127 chemistry of quartz in granitic pegmatites of Southern Norway: Petrogenetic and economic
1128 implications. *Economic Geology* 110, 1737–1757.
- 1129 Murphy J.B., Keppie J.D., Nance R.D., and Dostal J., 2010. Comparative evolution of the Iapetus and
1130 Rheic oceans: A North American perspective; *Gondwana Research*, Vol. 17, 482-499.
- 1131 Nance R.D., Gutiérrez-Alonso G., Keppie J.D., Linnemann U., Murphy J.B., Quesada C., Strachan -
1132 R.A., and Woodcock N.H., 2012. A brief history of the Rheic Ocean; *Geoscience Frontiers*, Vol. 3,
1133 125-135.
- 1134 Neace E.R., Nance R.D., Murphy J.B., Lancaster P.J., and Shail R.K., 2016. Zircon La-ICPMS
1135 geochronology of the Cornubian Batholith, SW England; *Tectonophysics*, Vol. 681, 332-352.
- 1136 Nicholson K., and Anderton R., 1989. The Dalradian rocks of the Lecht, NE Scotland: Stratigraphy,
1137 faulting, geochemistry and mineralization; *Transactions of the Royal Society of Edinburgh; Earth*
1138 *Sciences*, Vol. 80, 143-157.
- 1139 Nironen M., 1997. The Svecofennian Orogen: A tectonic model; *Precambrian Research*, Vol. 86, 21-
1140 44.
- 1141 Nishiyama T., Shimoda S., Shimosaka K., and Kanaoka S., 1975. Lithium-bearing tosudite; *Clays and*
1142 *Clay Minerals*; Vol. 23, 337-342.
- 1143 Norton J.J. 1973. Lithium, cesium, and rubidium—the rare alkali metals (United States Mineral
1144 Resources), USGS Professional Paper 820, 363-378.

- 1145 Novák M., and Povondra P., 1995. Elbaite pegmatites in the Moldanubicum: A new subtype of the
1146 rare-element class; *Mineral. Petrol.*, Vol. 12, 159-176.
- 1147 Novák M., Černý P., Kimbrough D.L., Taylor M.C., and Ercit T.S., 1998. U-Pb ages of monazite from
1148 granitic pegmatites in the Moldanubian Zone and their geological implications; *Acta Universitatis
1149 Carol Geologica*, Vol. 42, 309-310.
- 1150 Obradovic J., Djurdjevic-Colson J., and Vasic, N., 1997. Phytogenic lacustrine sedimentation –oil
1151 shales in Neogene from Serbia Yugoslavia; *Journal of Paleolimnology*, Vol. 18, 351-364.
- 1152 PANNN, 2017. Estudo de impacte ambiental mina da argemela; Proposta de definição de âmbito,
1153 134 p.
- 1154 Petrik I., Cik S., Miglierini M., Vaculovic T., Dianiska I., and Ozdin D., 2014. Alpine oxidation of
1155 lithium micas in Permian S-type granites (Gemic unit, Western Carpathians, Slovakia);
1156 *Mineralogical Magazine*, Vol. 78, 507-533.
- 1157 Piantone P., Wu X., and Touray J.C., 1994. Zoned hydrothermal alteration and genesis of the gold
1158 deposit at Le Châtelet (French Massif Central); *Economic Geology*, Vol. 89, 757-777.
- 1159 Polgari M., Philippe M., Szabo-Drubina M., and Toth M., 2005. Manganese-impregnated wood from a
1160 Toarcian manganese ore deposit, Eplény mine, Bakony Mts., Transdanubia, Hungary; *Neues Jahrbuch
1161 fur Geologie und Paläontologie Monatshefte*, Vol. 3, 175-192.
- 1162 Raimbault L., and Burnol L., 1998. The Richemont rhyolitic dyke, Massif Central, France: A
1163 subvolcanic equivalent of rare-metal granite; *The Canadian Mineralogist*, Vol. 36, 256-282.
- 1164 Raimbault L., Cuney M., Azencott C., and Duthou J.L., 1995. Geochemical evidence for a multistage
1165 magmatic genesis of Ta-Sn-Li mineralization in the granite de Beauvoir, French Massif Central;
1166 *Economic Geology*, Vol. 90, 548-76.
- 1167 Ramos J.F., Ribeiro A., and Barriga F.J.A.S., 1994. Mineralizações de metais raros de Seixo Amarelo-
1168 Gonçalo (Guarda); *Bol Minas*, Vol. 31, 101-115.
- 1169 Rio Tinto, 2017. Notice to ASX, Increase to Jadar Project Mineral Resources, 2 March 2017, 22 p.
1170 http://www.riotinto.com/documents/170302_Increase_to_Jadar_Project_Mineral_Resources.pdf
- 1171 Roberts N.M.W., and Slagstad T., 2015. Continental growth and reworking on the edge of the
1172 Columbia and Rodinia supercontinents; 1.86-0.9 Ga accretionary orogeny in southwest Fennoscandia;
1173 *International Geology Review*, Vol. 57, 1582-1606.
- 1174 Roda-Robles E., Pesquera A., Gil-Crespo P.P., Vieira R., Lima A., Garate-Olave I., Martins T., and
1175 Torres-Ruiz J., 2016. Geology and mineralogy of Li-mineralization in the Central Iberian Zone (Spain
1176 and Portugal); *Mineralogical Magazine*, Vol. 80, 103-126.

- 1177 Roda-Robles E., Vieira R., Pesquera A., and Lima A., 2010. Chemical variations and significance of
1178 phosphates from the Fregeneda-Almendra pegmatite field, Central Iberain Zone (Spain and Portugal);
1179 *Mineralogy and Petrology*, Vol. 100, 23-34.
- 1180 Roda-Robles E., Vieira R., Lima A., and Pesquera-Pérez A., 2009. Petrogenetic links between granites
1181 and pegmatites in the Fregeneda-Almendra area (Salamanca, Spain and Guarda, Portugal): New
1182 insights from $^{40}\text{Ar}/^{39}\text{Ar}$ dating in micas; *Estudos Geologicos*, Vol. 19, 305-310.
- 1183 Romer R.L., and Kroner U., 2015. Phanerozoic tin and tungsten mineralization – Tectonic controls on
1184 the distribution of enriched protoliths and heat sources for crustal melting; *Gondwana Research*, Vol.
1185 31, 60-95.
- 1186 Romer R.L., Kirsch M., and Kroner U., 2011. Geochemical signature of Ordovician Mn-rich
1187 sedimentary rocks on the Avalonian shelf; *Canadian Journal of Earth Sciences*, Vol. 48, 703-718.
- 1188 Romer R.L., Förster H.J., and Štemprok M., 2010. Age constraints for the Late-Variscan magmatism
1189 in the Altenberg-Teplice caldera (eastern Erzgebirge, Krušné hory); *Neues Jahrbuch für Mineralogie*
1190 *Abhandlungen*, Vol. 187, 289-305. [https:// doi .org /10 .1127 /0077 -7757 /2010 /0179](https://doi.org/10.1127/0077-7757/2010/0179).
- 1191 Romer R.L., and Smeds S.A., 1997. U-Pb columbite chronology of post-kinematic Palaeoproterozoic
1192 pegmatites in Sweden; *Precambrian Research*, Vol. 82, 85-99.
- 1193 Romer R.L., Schärer U., and Steck A., 1996. Alpine and pre-Alpine magmatism in the root-zone of the
1194 western Central Alps; *Contributions to Mineralogy and Petrology*, Vol. 123, 138–158.
- 1195 Romer R.L., and Smeds S.A., 1994. Implications of U-Pb ages of columbite-tantalites from granitic
1196 pegmatites for the Paleoproterozoic accretion of 1.90-1.85 Ga magmatic arcs to the Baltic Shield;
1197 *Precambrian Research*, Vol. 67, 141-158.
- 1198 Romer R.L., and Wright J.E., 1992. U-Pb dating of columbite - A geochronologic tool to date
1199 magmatism and ore deposits; *Geochimica et Cosmochimica Acta*, Vol. 56, 2137–2142.
- 1200 Roskill Information Services Ltd., 2016. Lithium: Global Industry, Markets and Outlook to 2025;
1201 Thirteenth Edition. London.
- 1202 Rudnick R.L., and Gao S., 2004. Composition of the continental crust; *In* *Treatise on Geochemistry*,
1203 Holland H.D., and Turekian K.K. (eds.); Elsevier, Amsterdam; Vol. 3, 1-64.
- 1204 Scherer E., Mücke C., and Mezger K., 2001. Calibration of the lutetium-hafnium clock; *Science*, Vol.
1205 293, 683-687.
- 1206 Schmid S.M., Bernoulli D., Fügenschuch B., Matenco L., Schefer S., Schuster R., Tischler M., and
1207 Ustaszewski K., 2008. The Alpine-Carpathian-Dinaridic orogenic system: Correlation and evolution
1208 of tectonic units; *Swiss Journal of Geosciences*, Vol. 101, 139-183.

- 1209 Schuster R., and Stüwe K., 2008. The Permian metamorphic event in the Alps; *Geology*, Vol. 36/8,
1210 303-306.
- 1211 Shengsong Y., 1986. The hydrochemical features of salt lakes in Qaidam basin; *Chinese Journal of*
1212 *Oceanology and Limnology*, Vol. 4, 383–403.
- 1213 Silva D., Lima A., Gloaguen E., Gumiaux C., Noronha F., and Deveaud S. 2018. Chapter 3 - Spatial
1214 geostatistical analysis applied to the Barroso-Alvão rare-elements pegmatite field (Northern Portugal).
1215 *In* Teodoro A.C. (ed.), *Frontiers in Information Systems, GIS an Overview of Applications*, Bentham
1216 Science Publishers, Sharjah, UAE, 1:67-101.
- 1217 Simić V., Andrić N., Životić D., and Rundić L., 2017. Evolution of Neogene Intramontane basins in
1218 Serbia; Pre-meeting Field trip B1 Abstract, 1 p.
- 1219 Smolin A., and Beaudry C., 2015. Mineral opportunities in Ukraine; 3rd Conference on Raw Materials;
1220 European Innovation Partnership on Raw Materials, Presentation.
- 1221 Stanley C., Jones G.C., Rumsey M.S., Blake C., Roberts A.C., Stirling J.A.R., Carpenter G.J.C.,
1222 Whitfield P.S., Grice J.D., and Lepage Y., 2007. Jadarite, $\text{LiNaSi}_3\text{B}_3\text{O}_{10}(\text{OH})$, a new mineral species
1223 from the Jadar Basin, Serbia; *European Journal of Mineralogy*, Vol. 19, 575-580.
- 1224 Štemprok M., Pivec E., and Langrova A., 2005. The petrogenesis of a wolframite-bearing greisen in
1225 the Vykamov granite stock, Western Krusné Hory pluton (Czech Republic); *Bulletin of Geosciences*,
1226 Vol. 80, 163-184.
- 1227 Stewart, D.B., 1978, Petrogenesis of lithium-rich pegmatites: *American Mineralogist*, Vol. 63, 970–
1228 980.
- 1229 Stojadinovic U., Matenco L., Andriessen P., Toljic M., Rundic L., and Ducea M., 2017. Structure and
1230 provenance of Late Cretaceous-Miocene sediments located near the NE Dinarides margin:
1231 Interferences from kinematics of orogenic building and subsequent extensional collapse;
1232 *Tectonophysics*, Vol. 710-711, 184-204.
- 1233 Suikkanen E., Huhma H., Kurhila M., and Lahaye Y., 2014. The age and origin of the Vaasa
1234 migmatite complex revisited; *Bulletin of the Geological Society of Finland*; Vol. 86, 41-55.
- 1235 Szabo Z., Grasselly G., and Cseh-Németh J., 1981. Some conceptual questions regarding the origin of
1236 manganese in the Urkut deposit, Hungary; *Chemical Geology*, Vol.34, 19-29.
- 1237 Tarascon J.M., 2010. Is lithium the new gold?; *Nature Chemistry*, Vol. 2, 510.
- 1238 Thöni M., Miller Ch., Zanetti A., Habler G., and Goessler W., 2008. Sm-Nd isotope systematics of
1239 high-REE accessory minerals and major phases: ID-TIMS, LA-ICP-MS and EPMA data constrain

- 1240 multiple Permian-Triassic pegmatite emplacement in the Koralpe, Eastern Alps; *Chemical Geology*,
1241 Vol. 254, 216-237.
- 1242 Thöni M., and Miller C., 2000. Permo-Triassic pegmatites in the eo-Alpine eclogite facies Koralpe
1243 complex, Austria: Age and magma source constraints from mineral, chemical, Rb-Sr and Sm-Nd
1244 isotope data; *Schweizerische Mineralogische und Petrographische Mitteilungen*, Vol. 80, 169-186.
- 1245 Tomljenovic B., 2002. *Strukturne Znacajke Medvednice i Samoborskoj gorja*; PhD thesis, University
1246 of Zagreb, 208 p.
- 1247 Tourtelot H.A., and Brenner-Tourtelot E.F., 1977. Lithium, a preliminary survey of its mineral
1248 occurrence in flint clay and related rock types in the United States; *Energy*, Vol. 3, 263-272.
- 1249 Uher P., Chudik P., Bacik P., Vaculovic T., and Galiova M., 2010. Beryl composition and evolution
1250 trends: an example from granitic pegmatites of the beryl-columbite subtype, Western Carpathians,
1251 Slovakia; *Journal of Geosciences*, Vol. 55, 69-80.
- 1252 Van Breemen O., Bowes D.R., Aftalion M., and Żelaźniewicz A., 1988. Devonian tectonothermal
1253 activity in the Sowie Gory Gneissic Block, Sudetes, Southwestern Poland: Evidence from Rb-Sr and
1254 U-Pb isotopic studies; *Annales Societatis Geologorum Poloniae*, Vol. 58, 3-19.
- 1255 Van Lichtenvelde M., Grand'Homme A., de Saint-Blanquat M., Olivier P., Gerdes A., Paquette J.L.,
1256 Melgarejo J.C., Druguet E., and Alfonso P., 2017. U-Pb geochronology on zircon and columbite-
1257 group minerals of the Cap de Creus pegmatites, Spain; *Mineralogy and Petrology*, Vol. 111, 1-21.
- 1258 Viallette M.Y., 1963. Ages absolus par méthode au strontium des lépidolites du Massif Central
1259 français; *Comptes rendus du 88eme congrès national des sociétés savantes, Clermont Ferrand, Section*
1260 *des Sciences*, 17 p.
- 1261 Vieira R., Roda-Robles E., Pesquera A., and Lima, A., 2011. Chemical variation and significance of
1262 micas from the Fregeneda-Almendra pegmatitic field (Central-Iberian Zone, Spain and Portugal);
1263 *American Mineralogist*, Vol. 96, 637-645.
- 1264 Vieira R., 2010. *Aplitopegmatitos com elementos raros da região entre Almendra (V. N. de Foz-Côa)*
1265 *e Barca d'Alba (Figueira de Castelo Rodrigo). Campo plitopegmatítico da Fregeneda-Almendra*; PhD
1266 Thesis, University of Porto, Portugal, 275 p.
- 1267 Vignola P., Diella V., Oppizi P., Tiepolo M., and Weiss S., 2008. Phosphate assemblages from the
1268 Brissago granitic pegmatite, western Southern Alps, Switzerland; *The Canadian Mineralogist*, Vol. 46,
1269 635-650.
- 1270 Vinogradov A.P., and Tugarinov A.I., 1961. The geologic age of pre-Cambrian rocks of the Ukrainian
1271 and Baltic shields; *Annals of the New York Academy of Sciences*, Vol. 91, 500-513.

- 1272 Yaksic A., and Tilton J.E., 2009. Using the cumulative availability curve to assess the threat of
1273 mineral depletion: The case of lithium; *Resources Policy*, Vol. 34, 185-194
- 1274 Yu J., Gao C., Cheng A., Liu Y., Zhang L., and He X., 2013. Geodynamic, hydroclimatic and
1275 hydrothermal controls on the formation of lithium brine deposits in the Qaidam Basin, northern
1276 Tibetan Plateau, China; *Ore Geology Reviews*, Vol. 50, 171-183.
- 1277 Waldron J.W.F., Schofield D.I., White C.E., and Barr S.M., 2011. Cambrian successions of the
1278 Meguma Terrane, Nova Scotia and Harlech Dome, North Wales: dispersed fragments of a peri-
1279 Gondwana basin?; *Journal of the Geological Society*, Vol. 168, 83-97.
- 1280 White C.E., 2008. Defining the stratigraphy on the Meguma Supergroup in southern Nova Scotia;
1281 Where do we go from here?; *Atlantic Geology*, Vol. 44, 58 p.
- 1282 Woodcock N.H., Soper N.J., and Strachan R.A., 2007. A Rheic cause for the Acadian deformation in
1283 Europe; *Journal of the Geological Society, London*, Vol. 167, 1023-1036.
- 1284 Wang D.H., Li P.G., Qu W.J., Yin L.J., Zhao Z., Lei Z.Y., and Wen S.F., 2013. Discovery and
1285 preliminary study of the high tungsten and lithium contents in the Dazhuyuan bauxite deposit,
1286 Guizhou, China. *Science China; Earth Sciences*, Vol. 56, 145–152. doi: 10.1007/s11430-012-4504-2
- 1287 Zasedatelev, A.M. 1977. Quantitative model of metamorphic generation of rare-metal pegmatite with
1288 lithium mineralization: *Doklady Akademii Nauk SSSR, seria geologicheskaya*, Vol. 236, 219–221.
- 1289 Zelazniewicz A., Cwojdzinski S., England R. W., and Zientara P., 1997. Variscides in the Sudetes and
1290 the reworked Cadomian orogeny: evidence from the GB-2A seismic reflection profiling in
1291 southwestern Poland; *Geological Quarterly*, Vol. 41, 289-308.
- 1292 Zhang R., Lehmann B., Seltmann R., Sun W., and Li C., 2017. Cassiterite U-Pb geochronology
1293 constrains magmatic-hydrothermal evolution in complex evolved granite systems: The classic
1294 Erzgebirge Tin Province (Saxony and Bohemia); *Geology*, Vol. 45, 1096-1098.
- 1295 Zhao G., Cawood P.A., Wilde S.A., and Sun M., 2002. Review of global 2.1-1.8 Ga orogens:
1296 Implications for a pre-Rodinia supercontinent; *Earth Science Reviews*, Vol. 59, 125-162.
- 1297 Ziemann S., Weil M., and Schebek L., 2012. Tracing the fate of lithium—The development of a
1298 material flow model; *Resources, Conservation and Recycling*, Vol. 63, 26-34.

1299

1300 **8. Table captions**

1301 Table 1: Main Li-bearing minerals encountered in Europe, their corresponding chemical formula, Li
1302 content (Li_2O and Li metal) and physical characteristics.

1303

1304 Table 2: RMG classification according to Linnen and Cuney (2005) with European examples.

1305

1306 Table 3: Pegmatite classification according to Černý and Ercit (2005) and Černý et al. (2012) and
 1307 corresponding P/T conditions. LCT pegmatites in red show a significant lithium potential and those in
 1308 orange a moderate lithium potential, with corresponding examples if known. LCT = lithium-cesium-
 1309 tantalum; NYF = niobium–yttrium–fluorine.

1310

1311 Table 4: Li projects in Europe and their past production and estimated Li metal resources/reserves. NA
 1312 refers to data not available. (data were collected from exploration and mining companies; Lulzac and
 1313 Apolinarski, 1986; Smolin and Beaudry, 2015; British Geological Survey, 2016)

1314

1315 Table 5: Location and dating of several pegmatites, RMG and greisen deposits in Europe

1316

1317 9. Figure captions

1318 Figure 1. Cross sections of various lithium deposits. Lithium-bearing units are identified in red in each
 1319 section. A) Beauvoir RMG (France) and related stockwork (modified from Cuney and Autran, 1987).
 1320 B) Sepeda pegmatite in Portugal (modified from Dakota Minerals, 2017); pink area represents barren
 1321 pegmatite. C) Cinovec deposit in Czech Republic (modified from Breiter et al., 2017). D) Jadar Basin
 1322 in Serbia and location of the jadarite layers (modified from Rio Tinto, 2017). **Color should be used**

1323

1324 Figure 2. Photographs of various styles of lithium mineralization. A) Quartz-feldspar and zinnwaldite
 1325 mineralization (Podlesi, Czech Republic). B) Greisen and related La Bosse stockwork (Beauvoir,
 1326 Massif Central, France). C) Montebras stocksheider hosted in RMG (Massif Central, France).
 1327 D) Phenocrysts of petalite (yellowish-greenish minerals) surrounded by purplish lepidolite in quartz-
 1328 potassic feldspar-albite matrix (Chédeville pegmatite, Massif Central, France). E) Alternating
 1329 lepidolite-rich and aplite-rich layers in a horizontal pegmatite (Chédeville pegmatite, Massif Central,
 1330 France). Scale represents 7 cm. Abbreviations: Lpd: lepidolite; Ptl: petalite; Znw: Zinnwaldite;
 1331 Qz+Fsp: quartz+feldspar. F) Jadarite mineralization (Jadar Basin, Serbia) in mudstone (courtesy of
 1332 Matevž Novak, Geological Survey of Slovenia) **Color should be used**

1333

1334 Figure 3. A) Schematic map of the East European Craton and distribution of the main shields
1335 (modified after Roberts and Slagstad, 2015). The red box highlights the studied area. B) Simplified
1336 geological map of the Fennoscandian Shield (modified after Koistinen et al., 2001 and Bergh et al.,
1337 2015) showing distribution of the Svecofennian and the Sveconorwegian orogens, and distribution of
1338 LCT and mixed NYF-LCT pegmatites. Red circles and surrounded red names refer to LCT pegmatite
1339 fields; blue circle and name refer to mixed NYF-LCT pegmatite field; n = number of identified
1340 pegmatite bodies. Abbreviations: B: Bamble Terrane; ES: Eastern Segment; I: Idefjorden Terrane; T:
1341 Telemark Terrane; SFDZ: Sveconorwegian Frontal Deformation Zone. **Color should be used**

1342
1343 Figure 4. Simplified geological map of the crustal block involved in the Caledonian orogeny along the
1344 Rhenic Suture and location of contemporaneous Mn-(Fe) rich deposits (modified after Linnemann et
1345 al., 2007; Garfunkel, 2015). Note that Caledonian relics within Gondwana were reworked during the
1346 Variscan and Alpine orogenies making reconstruction of their respective contacts difficult. **Color**
1347 **should be used**

1348
1349 Figure 5. A) Schematic map of the Mid-Devonian paleo-continental reconstruction (modified after
1350 Woodcock et al., 2007). Red box highlights studied area. B) Simplified geological map of Ireland and
1351 northern Britain with distribution of LCT pegmatites related to the Caledonian orogeny (modified after
1352 Miles et al., 2016). Red circle and surrounded red name refer to Leinster LCT pegmatite fields from
1353 which nine LCT pegmatites are identified. **Color should be used**

1354
1355 Figure 6. Simplified geological map of the Variscan orogeny in Europe, location of various lithium-
1356 bearing deposits and a selection of ages (modified after Murphy et al., 2010; Martínez Catalán, 1990).
1357 Note that the Variscan orogeny was subsequently reworked along the Alpine Front by the Alpine
1358 orogeny. Additionally, 260 Li-rich bodies including LCT pegmatites, greisen and the Argemela RMG
1359 are identified in Portugal and Spain, 50 Li-rich occurrences are identified in the Bohemian Massif and
1360 26 LCT pegmatites are identified in South Austria. Abbreviations: AM: Armorican Massif; AVZ:
1361 Arveno-Vosgina Zones; BM: Bohemian Massif; CAZ: Central Armorican Zone; CIZ: Central Iberian
1362 Zone; CZ: Cantabrian Zone; GTMZ: Galicia-Tras-os-Montes Zone; MZ: Moldanubian Zone; NAZ:
1363 North Armorican Zone; OS: Ossa-Morena Zone; RM: Rhenish Massif; SAZ: South Armorican Zone;
1364 SPZ: South Portugese Zone; SZ: Saxothuringian Zone; TBZ: Tepla-Barradian Zone; WALZ: West
1365 Asturian-Leonese Zone. **Color should be used**

1366
1367 Figure 7. Simplified geological map of the Alpine-Mediterranean area and location of lithium-bearing
1368 deposits (modified after Tomljenovic, 2002; Bousquet et al., 2012). Brissago and Elba Islands

1369 pegmatite fields are highlighted by a red circle; black circle is Dauphinois region with cookeites; *n*
1370 suggests number of identified pegmatite bodies. Abbreviations: BM: Bohemian Massif; EA: Eastern
1371 Alps; EC: East Carpathians; IWC: Internal West Carpathians; NCA: Northern Calcareous Alps; SC:
1372 South Carpathians. Color should be used

1373

1374 Figure 8. Simplified geotectonic map of Europe (modified after Artemieva et al., 2006; Charles et al.,
1375 2013) and distribution of various Li-bearing occurrences. Color should be used

1376

1377 Figure 9. Location map of the Li deposits (Table 4) in Europe (modified after Artemieva et al., 2006;
1378 Charles et al., 2013). Categories refer to: A $\geq 1,000,000$ t Li₂O; 1,000,000 t \geq Category B $\geq 100,000$ t
1379 Li₂O; 100,000 t \geq Category C $\geq 50,000$ t Li₂O; 50,000 t \geq Category D $\geq 5,000$ t Li₂O; Category E
1380 $< 5,000$ t Li₂O and past production and mineral resources. Color should be used

1381

1382 Figure 10. Geological sections of favorable lithium setting. Continental collision (A; modified from
1383 Menant et al., 2018) shifting to post-collision setting (B; modified from Menant et al., 2018)
1384 represents favorable context for Li-hard-rock formation such as LCT pegmatites, RMG and greisen
1385 along orogenic collapse (C). Superscripts on C correspond to European examples: ¹ = Chédeville,
1386 Mina Feli, or Gonçalo; ² = Richemont; ³ = Beauvoir, Argemela and Montebras; ⁴ = Barroso-Alvao,
1387 Lântta and Aclare. Continental subduction (D; modified from Menant et al., 2018) shifting to back-arc
1388 setting (E; modified from Menant et al., 2018) represents favorable context for
1389 sedimentary/hydrothermal Li deposits such as Jadar (F; modified from Stojadinovic et al., 2016). LCT
1390 pegmatite can also occur in such a context. Color should be used

1391

1392 Figure 11. Average lithium grade (wt.% Li₂O) *versus* metric tons of ore (Mt) for the 28 identified Li
1393 deposits in Europe regarding their deposit type. Deposits and projects based on historical estimates are
1394 written in italics and those based on the CRIRSCO system in bold. The Whabouchi (Canada; blue
1395 triangle) and Greenbushes (Australia; green triangle) pegmatite deposits are mentioned here in order to
1396 compare these world-class deposits to European grades and tonnages. Color should be used

1397

1398 Figure 12. Grade (wt.% Li₂O) *versus* deposit types (A) and deposit tonnage (Mt) *versus* deposit types
1399 (B) considering resource estimates. The boxes indicate the median (black line), upper and lower
1400 quartiles (25%; gray boxes), maximum and minimum values (upper and lower whiskers) and outliers
1401 (black circles). Note that *n* reflects the total number of deposits considered for this summary plot.

1402